

DEPARTMENT OF GEOSCIENCE AND PETROLEUM

TPG4851 - HALTENBANKEN CO2 REDUCTION VILLAGE

---

## Project Report

---

GROUP 6

*Authors:*

Ştefan Cătălin Crăciun  
Tilla Farnes Hennum  
Vegard Berge  
Kiane Rezaei

May, 2022

---

# Table of Contents

<b>List of Figures</b>	<b>iii</b>
<b>List of Tables</b>	<b>iii</b>
<b>1 Introduction</b>	<b>1</b>
<b>2 The Haltenbanken Field</b>	<b>2</b>
2.1 Geological Overview . . . . .	2
2.2 The Fields . . . . .	3
2.2.1 Skuld . . . . .	3
2.2.2 Norne . . . . .	3
2.2.3 Alve . . . . .	3
2.2.4 Marulk . . . . .	4
2.2.5 Skarv . . . . .	4
2.2.6 Heidrun . . . . .	4
2.2.7 Åsgard . . . . .	4
2.2.8 Morvin . . . . .	5
2.2.9 Kristin . . . . .	5
2.2.10 Yttergryta . . . . .	5
2.2.11 Tyrihans . . . . .	5
2.2.12 Mikkel . . . . .	6
2.2.13 Draugen . . . . .	6
2.2.14 Njord . . . . .	6
2.2.15 Hyme . . . . .	6
2.3 Total Hydrocarbon Production . . . . .	7
2.4 CO <sub>2</sub> Emissions . . . . .	8
<b>3 General Solution</b>	<b>10</b>
<b>4 Windmill Farm</b>	<b>11</b>
4.1 Placement . . . . .	11
4.2 Energy Storage . . . . .	12
<b>5 Hydrogen Production</b>	<b>13</b>
5.1 Methods . . . . .	13
5.1.1 Steam Methane Reforming . . . . .	13

---

5.1.2	Autothermal Reforming	13
5.1.3	Comparison	14
5.2	Design	14
5.2.1	Carbon Removal	15
5.3	Calculations	16
5.3.1	Energy Demand	16
5.3.2	Facility	17
<b>6</b>	<b>Carbon Capture and Storage</b>	<b>17</b>
6.1	CCS in Norwegian Sea	17
6.2	Aquifers	18
6.2.1	The Åre and Tilje	19
6.2.2	The Ile and Garn	20
6.3	The Rogn formation	21
6.4	Depleted Reservoirs	21
6.5	Decision	21
6.6	Well design	22
6.7	Monitoring plan	22
<b>7</b>	<b>Transportation</b>	<b>23</b>
7.1	Hydrogen Transportation	23
7.2	CO <sub>2</sub> transportation	25
<b>8</b>	<b>Economy</b>	<b>26</b>
8.1	Windmill Farm	28
8.2	Hydrogen Production	28
8.3	CCS	29
8.4	Income	29
<b>9</b>	<b>Conclusion</b>	<b>29</b>
<b>Bibliography</b>		<b>31</b>
<b>Appendix</b>		<b>35</b>
A	Infrastructure in the Haltenbanken Area	35
B	Lithostratigraphy of the Haltenbanken Area	36
C	Calculations - Excel	37
D	Tables and Images regarding CCS	39

---

---

E	Table of Estimated Costs and Income	42
---	-------------------------------------	----

## List of Figures

1	Haltenbanken Area	2
2	Production	7
3	Total Production in the Haltenbanken area from 1997 to 2020 in Sm3 oil equivalents. All data are compiled from NPD website.	8
4	Total CO <sub>2</sub> emission in the Haltenbanken area from 1997 to 2020 in 1000 of tonnes. All data are compiled from NPD website.	9
5	Total CO <sub>2</sub> emission in the Haltenbanken area from 1997 to 2020 in 1000 of tonnes. All data are compiled from NPD website.	9
6	Illustration of the proposed solution.	10
7	FLASC concept.	12
8	Block Flow Diagram of Conventional SMR Process Plant with Carbon Removal.	14
9	Block Flow Diagram of Shift & Syngas Conditioning.	15
10	The Tjile/Åre aquifer	19
11	The Ile/Garn Aquifer	20
12	The late Jurassic Rogn Formation.	21
13	Illustration of the proposed hydrogen pipeline network. The distances in the illustration are not to scale.	24
14	Transportation cost comparison - "Ship vs Pipeline".	26
15	Distance between our Capture Point and the injection site.	26
16	Distribution of CAPEX and OPEX in the project.	27
17	Development of NPV throughout a lifetime of 20 years.	28
18	Infrastructure of the Halten Terrace.	35
19	General stratigraphy and hydrocarbon occurrences of the Halten Terrace.	36
20	Energy content of hydrogen.	37
21	Energy demand for methane conversion.	38
22	General stratigraphy of the Norwegian Sea.	39
23	Overview of calculation of the estimated costs and income, in MNOK (2022).	43

## List of Tables

1	Energy demand for transformation of 30% of the natural gas to hydrogen.	11
2	Characteristics - LHV.	16
3	Characteristics - HHV.	16

---

4	SMR parameters. . . . .	16
5	SMR - Mass and volume flows. . . . .	16
6	Daily energy demand. . . . .	17
7	The summary of well design. . . . .	22
8	Summary of the proposed monitoring plan. . . . .	23
9	Estimated length of hydrogen transport pipeline network. Measured distances is taken from maps from NPD. . . . .	25
10	Typical conditions and properties across the shipping chain and pipeline. Data are compiled from the source. . . . .	25
11	The Tjile/Are Aquifer Features. . . . .	40
12	The Garn/Ile Aquifer Features. . . . .	40
13	Parameters used in the well design. All data are compiled from NPD website. . . . .	41
14	Results for the well design. . . . .	41
15	Calculated CAPEX and OPEX, in MNOK (2022). . . . .	42

---

## 1 Introduction

Nowadays we face a climate and energy challenge that needs to be addressed as quickly as possible. In order to comply with the 2015 Paris Agreement we need to find better and innovative ways that tackle emission reductions in accordance with the best available science to achieve a balance between manmade emissions and affordable energy, while making a profit at the same time.

Attaining the Paris Agreement's most ambitious targets now necessitates swift, deep, and long-term reductions in global greenhouse gas emissions. This includes a 45 percent reduction in global carbon dioxide emissions by 2030 compared to 2010 levels, and a net zero by mid-century, as well as significant reductions in other greenhouse gases like methane. The Pact also emphasizes the need of safeguarding, conserving, and restoring the environment and ecosystems, as well as the need for a rapid scale-up and deployment of clean power generation and energy-efficiency measures [1].

While the need to address climate change is apparent, so is the world's economy's dependence on reliable and affordable energy. Fast-growing developing nations are navigating a period of urbanisation and industrialisation that has historically been energy and carbon heavy. When energy markets are out of balance, as seen in late 2021 and early 2022 (due to the COVID19 pandemic), developed countries have gone through shocks and dislocations, resulting in personal, political, and economic implications. Governments, businesses, investors, and individuals will have to strike a delicate and challenging balance between guaranteeing quick emission reductions and assuring the continuous provision of reliable and inexpensive energy as they take on the urgent issue of getting to net zero emissions.

The world will need to manage the risks of a disorderly transition while trying to limit the threats of climate change. The energy transition will require governments to make bold policy decisions in order for it to succeed. It will necessitate corporations taking new risks and investors supporting them in doing so. It will necessitate certain changes in consumer behavior. Above all, success will necessitate collaboration, courage, trust, and a shared commitment [1].

This project aims to deal with some of the issues raised above. Here we propose an integrated solution that can offer companies and investors insight on how they can further develop and invest towards a future that aims to reduce the CO2 emissions related to the oil and gas industry (both direct and indirect emissions).

---

## 2 The Haltenbanken Field

### 2.1 Geological Overview

The Halten Terrace is located between the Trøndelag Platform and the Møre Basin on the mid-Norwegian continental shelf, as seen in Figure 1. The structure is represented by a broad fault terrace which contains a normal faulted pre-rift sequence draped by a syn-rift sequence of variable thickness and a thick post-rift sequence [2].

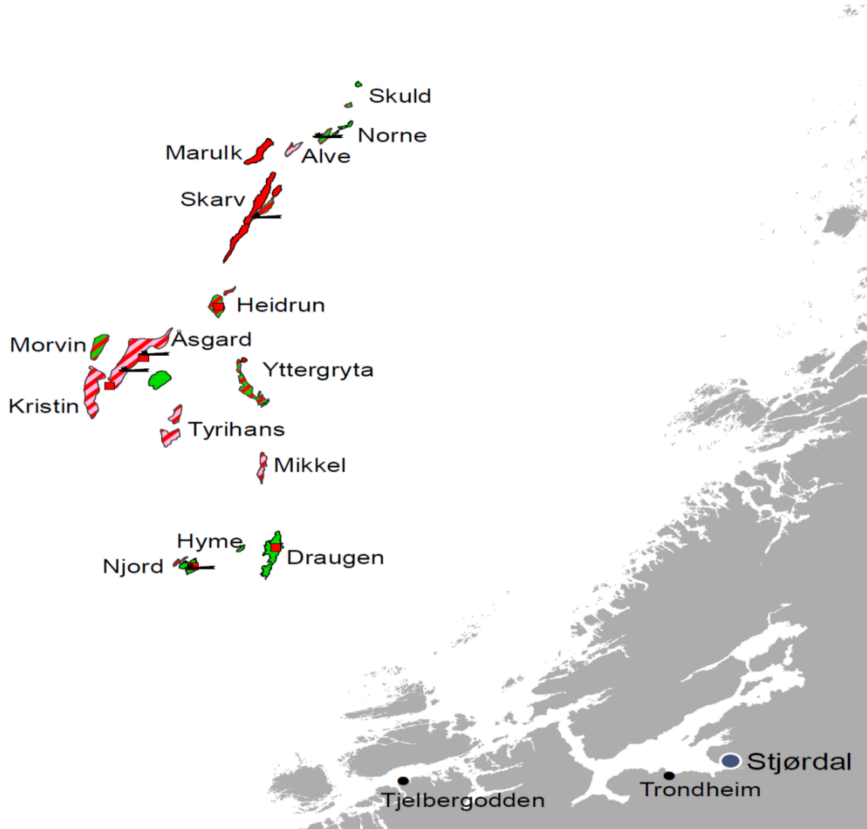


Figure 1: Haltenbanken Area.

Source: [3]

There are two source rocks that are of significant importance, namely: the mature Early Jurassic coal-bearing gas-condensate source rock and the Late Jurassic Spekk Formation oil source rock.

There are three main hydrocarbon plays:

The pre-rift play. This covers the northeastern fairway and contains some commercial fields. These are characterized by a hydrostatic reservoir pressure or low-grade overpressure. Moving to the West of the terrace, the reservoirs are found at a greater depth and have a big overpressure. In this area, exploration has been unsuccessful so far. This play has been thoroughly explored but there is still some potential for high-risk gas prospects in the overpressured Halten West area [2].

The second play is given by syn-rift reservoirs which are given in the form of submarine fan systems on the hanging-wall blocks of the Vingleia Fault Zone, which received erosion products from the uplifted Frøya High to the south. Shallow marine shoreline and offshore bar sands are present on the major tilted footwall blocks along the edge of the Frøya High (Draugen-Rogn Formation) and along the edge of the Sklinna High. This play is still in the early stages of exploration but the oil potential is considerable.

---

The final play (post-rift play) relies on stratigraphic trapping in post-rift, Lange, Lysing and Nise sands on the Sklinna Saddle and in the Grinna Graben, where the sands may have been distributed further southwest from the uplifted and truncated Nordland Ridge. A thin Lysing Formation is oil-bearing in the Smørbukk Sør area. The potential of the post-rift play has not yet been tested and the play is thought to have a considerable oil potential.

Exploration in the early and mid 1980's was focused on structural traps of the pre-rift play, which has yielded all the commercial fields except Draugen. As we can see, the area has numerous proven oil and gas reserves. In our study, we will focus on fifteen of these fields, namely: Skuld, Norne, Alve, Marulk, Skarv, Heidrun, Morvin, Kristin, Yttergryta, Tyrihans, Åsgard, Mikkel, Draugen, Hyme and Njord.

## 2.2 The Fields

The pipeline network for all the fields is shown in Figure 18 in Appendix A. The Lithostratigraphic column for the Haltenbanken area can be seen in Figure 19 in Appendix B.

### 2.2.1 Skuld

The recoverable reserves of the Skuld field have been estimated to be 90 million barrels of oil equivalents. Skuld is being developed at a depth of 350 meters using three standard subsea templates and is linked to the Norne production vessel, which is also producing for the Norne, Urd, Alve, and Marulk fields. The field produces oil from the Åre, Tofte, and Ile Formations, which are sandstones from the Early to Middle Jurassic period. The Fossekall and Domhap deposits make up the field. The reservoirs are located at a depth of 2,400-2,600 meters and feature minor gas caps. The reservoir quality is moderate to good.

Water injection provides pressure support for the field. Some of the wells are also equipped with gas lift, which allows them to operate at low reservoir pressure and high water cut. Regarding transportation, the well stream is sent to the Norne production, storage, and offloading vessel. The oil is offloaded to shuttle tankers together with the oil from the Norne field. The gas is transported by pipeline from the Norne vessel to the Åsgard field, and further via the Åsgard Transport System (ÅTS) to the Kårstø terminal [4].

### 2.2.2 Norne

The Norne field is 80 kilometers north of Heidrun field. The depth of the water is 380 meters. A production, storage, and offloading vessel (FPSO) is used to develop the field, which is connected to seven subsea templates. The Norne FPSO is connected to the Alve, Urd, Skuld, and Marulk fields. Norne produces oil and gas from Jurassic sandstone. Oil is mainly found in the Ile and Tofte Formations, and gas in the Not Formation. The reservoir lies at a depth of 2,500 metres and has good quality. The field is produced by water injection as the drive mechanism. The oil is loaded onto tankers for export. Gas export is made through a dedicated pipeline to the Åsgard field and via Åsgard Transport System to the Kårstø terminal [5].

### 2.2.3 Alve

Alve lies 16 kilometres southwest of the Norne field. The water depth is 370 metres. The infrastructure consists of a standard subsea template with four well slots and three production wells. Alve is tied to the Norne FPSO by a pipeline. Alve produces oil and gas from sandstone of Early and Middle Jurassic age in the Tilje, Not and Garn Formations. The reservoir lies at a depth of 3,600 metres and has moderate to good quality. The field is produced by pressure depletion. The oil is offloaded from the Norne FPSO and the gas is transported via the Norne pipeline to the Åsgard Transport System and further to the Kårstø terminal for export [6].

---

#### 2.2.4 Marulk

Marulk is located 25 kilometres southwest of the Norne field. The water depth is 370 metres. The field is developed with a subsea template tied-back to the Norne FPSO. Marulk produces gas from Cretaceous sandstone in the Lysing and Lange Formation. The reservoirs are located at a depth of 2,800 – 2,850 metres. Both reservoirs are in turbidite fans and have moderate to good quality. The field is produced by pressure depletion. The well stream is sent to the Norne FPSO for processing. The gas is then transported via the Åsgard Transport System to the Kårstø terminal [7].

#### 2.2.5 Skarv

Skarv is a field in the northern part of the Norwegian Sea, 35 kilometres southwest of the Norne field. The water depth is 350-450 metres. Skarv is a joint development of the Skarv, Idun, Ærfugl and Gråsel deposits. The development concept is a production, storage and offloading vessel (FPSO) with five subsea templates. Skarv produces gas and oil from Lower and Middle Jurassic sandstone in the Tilje, Ile and Garn Formations. The Garn Formation has good reservoir quality, while the Tilje Formation has relatively poor quality. The reservoirs are divided into several fault segments and lie at a depth of 3,300-3,700 metres. The field is produced with pressure support by gas injection and gas lift. The oil is offloaded to shuttle tankers, while the gas is transported to the Kårstø terminal in an 80-kilometre pipeline connected to the Åsgard Transport System [8].

#### 2.2.6 Heidrun

Heidrun is a field which is 30 kilometres northeast of the Åsgard field. The water depth is 350 metres. The field has been developed with a floating concrete tension-leg platform (TLP), installed over a large subsea template with 56 well slots. Heidrun produces oil and gas from Lower and Middle Jurassic sandstone in the Åre, Tilje, Ile and Garn Formations. The reservoir lies at a depth of 2,300 metres and is heavily faulted and segmented. The Ile and Garn Formations have good reservoir quality, while the Åre and Tilje Formations are more complex. The field is produced with pressure maintenance using water and gas injection in the Ile and Garn Formations. In the more complex parts of the reservoir, in the Åre and Tilje Formations, the main recovery strategy is water injection. Some segments are also produced by pressure depletion. The oil is loaded onto tankers and shipped to either the Mongstad terminal or to Tetney in the UK. The gas is transported by the Haltenpipe pipeline to the terminal at Tjeldbergodden and/or via the Åsgard Transport System to the Kårstø terminal [9].

#### 2.2.7 Åsgard

The Åsgard field includes the deposits Smørbukk, Smørbukk Sør and Midgard (Figure 18). The field has been developed with subsea wells tied-back to FPSO, Åsgard A. The development also includes Åsgard B, a floating, semi-submersible facility for gas and condensate processing. The gas centre is connected to a storage vessel for condensate, Åsgard C. The Åsgard facilities are an important part of the Norwegian Sea infrastructure. The Mikkel and Morvin fields are tied to Åsgard B for processing, and gas from Åsgard B is sent to the Tyrihans field for gas lift.

Åsgard produces gas and considerable amounts of condensate from Jurassic sandstone at depths of as much as 4850 metres. The reservoir quality varies in the different formations, and there are large variations in the reservoir properties between the three deposits. The Smørbukk deposit is in a rotated fault block and contains gas, condensate and oil in the Åre, Tilje, Tofte, Ile and Garn Formations. The Smørbukk Sør deposit contains oil, gas and condensate in the Tilje, Ile and Garn Formations. The Midgard gas deposits are divided into four structural segments with the main reservoir in the Ile and Garn Formations. Smørbukk is produced partly by pressure depletion and partly by injection of excess gas from the field. Smørbukk Sør is produced by pressure support from gas injection. Midgard is produced by pressure depletion. Oil and condensate are temporarily

---

stored at Åsgard A, then shipped to land by tankers. The gas is exported through the Åsgard Transport System to the terminal at Kårstø. The condensate from Åsgard is sold as oil [10].

### **2.2.8 Morvin**

Morvin resides 15 kilometres west of the Åsgard field. The water depth is 360 metres. The field is developed with two 4-slot subsea templates, tied to the Åsgard B facility. Morvin produces gas and oil from Jurassic sandstone in the Tilje, Tofte, Ile, Garn and Spekk Formations. The reservoirs lie in a rotated and tilted fault block at a depth of 4,500-4,700 metres. The field is produced by pressure depletion. The well stream from Morvin is transported by a heated, 20-kilometre pipeline to the Åsgard B facility for processing and further transport [11].

### **2.2.9 Kristin**

Kristin sits a few kilometres southwest of the Åsgard field. The water depth is 370 metres. The field is developed with four 4-slot subsea templates tied-back to a semi-submersible facility for processing. The Tyrihans field is tied to the Kristin facility.

Kristin produces gas and condensate from Jurassic sandstone in the Garn, Ile and Tofte Formations. The reservoirs lie at a depth of 4,600 metres and have high pressure and high temperature. The reservoir quality is generally good, but low permeability in the Garn Formation and flow barriers in the Ile and Tofte Formations contribute to a rapid decline in reservoir pressure. The field is produced by pressure depletion. The well stream is processed at Kristin and the gas is transported via the Åsgard Transport System to the Kårstø terminal. Light oil is transferred to the Åsgard C facility for storage and export. Condensate from Kristin is sold as oil [12].

### **2.2.10 Yttergryta**

Yttergryta is 33 kilometres east of the Åsgard B platform. The water depth is 300 metres. The field was developed with a subsea template connected to the Åsgard B platform via the Midgard X template. Yttergryta produced gas from sandstone of Middle Jurassic age in the Fangst Group. The reservoir is at a depth of 2,400-2,500 metres. The field was produced by pressure depletion. The gas was transported to the template Midgard X and further to the Åsgard B facility for processing. The gas from Yttergryta had a low CO<sub>2</sub> content, making it suitable for dilution of CO<sub>2</sub> in the Åsgard Transport System. Production ceased in 2011 because of water breakthrough in the gas production well [13].

### **2.2.11 Tyrihans**

Tyrihans is 25 kilometres southeast of the Åsgard field. The water depth is 270 metres. The field is developed with five subsea templates tied-back to the Kristin platform, four templates for production and gas injection and one template for seawater injection. Gas for injection and gas lift is supplied from the Åsgard B platform.

Tyrihans produces oil, gas and condensate from two deposits: Tyrihans Sør and Tyrihans Nord. Tyrihans Sør has an oil column with a condensate-rich gas cap. Tyrihans Nord contains gas and condensate with a thin oil zone. The main reservoir in both deposits is in the Middle Jurassic Garn Formation at a depth of 3500 metres. The reservoirs are homogenous and of good quality. In addition, one well produces oil from the Ile Formation. Tyrihans has earlier been produced with pressure support by water and gas injection. The main recovery strategy now is pressure depletion and gas cap expansion. The well stream is sent to the Kristin platform for processing. Gas is exported from Kristin via the Åsgard Transport System to the Kårstø terminal, while oil and condensate are transported by pipeline to the storage ship Åsgard C for export on shuttle tankers [14].

---

### 2.2.12 Mikkel

Mikkel is located 30 kilometres north of the Draugen field. The water depth is 220 metres. The field is developed with two subsea templates tied-back to the Åsgard B facility.

Mikkel produces gas and condensate from Jurassic sandstone in the Garn, Ile and Tofte Formations. The field consists of six structures separated by faults, all with good reservoir quality. It has a 300-metre thick gas/condensate column and a thin underlying oil zone. The reservoir depth is 2,500 metres. The field is produced by pressure depletion. The well stream from Mikkel is combined with the well stream from the Midgard deposit and routed to the Åsgard B facility for processing. The condensate is separated from the gas and stabilised before being shipped together with condensate from the Åsgard field. The condensate is sold as oil. The rich gas is transported via the Åsgard Transport System (ÅTS) to the Kårstø terminal for separation of the natural gas liquids (NGL). The dry gas is transported from Kårstø to continental Europe via the Europipe II pipeline [15].

### 2.2.13 Draugen

Draugen has been developed with a concrete fixed facility and integrated topside, and has both platform and subsea wells. Stabilised oil is stored in tanks at the base of the facility. Two pipelines connect the facility to a floating loading-buoy.

Draugen produces oil from two formations. The main reservoir is in sandstone of Late Jurassic age in the Rogn Formation. The western part of the field also produces from sandstone of Middle Jurassic age in the Garn Formation. The reservoirs lie at a depth of 1,600 metres. They are relatively homogeneous, with good reservoir quality. The field is produced by pressure maintenance from water injection and by aquifer support. The oil is offloaded via a floating loading-buoy and exported by tankers. The associated gas was earlier transported via the Åsgard Transport System to the Kårstø terminal, but is now used for power generation on the platform [16].

### 2.2.14 Njord

Njord is 30 kilometres west of the Draugen field. The water depth is 330 metres. Njord is developed with a floating steel platform unit, Njord A, containing drilling and processing facilities, and a storage vessel, Njord Bravo. The Hyme field is tied to the Njord facility. Produced oil was transported by pipeline to the storage vessel Njord Bravo, and further by tankers to the market. Gas from the field was exported through a 40-kilometre pipeline connected to the Åsgard Transport System and further to the Kårstø terminal. Production from the Njord field and its satellite field Hyme was temporarily shut down in 2016 because of Njord A structural integrity issues. Production from the Njord and Hyme fields is expected to resume in late 2022 [17].

### 2.2.15 Hyme

Hyme is 19 kilometres northeast of the Njord field. The water depth is 250 metres. The field is developed with a subsea template including one production well and one water injection well. Hyme is connected to the Njord A facility.

Hyme produces oil and gas from sandstone of Early and Middle Jurassic age in the Tilje and Ile Formations. The reservoir lies at a depth of 2,150 metres and has good quality. The field is produced with pressure support from seawater injection. The production well is equipped with gas lift. The well stream is transported to the Njord field and processed on the Njord A platform. The Njord facilities are used for both oil and gas export. Production stopped temporarily in 2016 when the Njord A facility was shut down and towed to land for reinforcement and modifications. Hyme is expected to resume production late 2022, when the Njord facility is in place again [18].

## 2.3 Total Hydrocarbon Production

Looking at the production history from 1997 to 2020 of all the fields we can see some clear trends with regards to the Gas, Oil, Condensate and NGL. Combining this with additional information related to the future development of some of these fields we can make some predictions of how the production will look like in the future.

The oil production is on a clear downtrend, as seen in Figure 2. After reaching a maximum production volume of 44.6 million Sm<sup>3</sup> oil equivalents in 2001, there has been a constant decline in the production, reaching 8.9 million Sm<sup>3</sup> oil equivalents in 2020. Continuing onwards we can expect this downtrend to continue for the next couple of years. Even if we consider that the Njord and Hyme fields will go back into operation at the end of 2022, they will have a minor contribution to the overall total production (as both Hyme and Njord produce a fairly low volume of oil). Since 1997 the Gas production has been increasing at an exponential rate until 2008. Since then, the production rate has been fairly constant, with a small uptrend until 2017, when it reached a maximum production of 23.7 million Sm<sup>3</sup> oil equivalents. With the Njord and Hyme field going back into production at the end of 2022 we can expect to continue this constant production rate to continue for the next couple of years.

One thing to consider is that there are many future fields planned to be developed in the Haltenbanken area as seen in Figure 18 in Appendix A. Some of them will make use of floating rigs such as the Aasta Hansteen, but most of the new fields will be produced using subsea templates. All of these will increase the production of oil and gas in the area, or at least maintain them constant at the current production values (as the old fields are being depleted, the new ones replace their production). A fair amount of the fields presented in the previous chapter will become depleted in the next decade if there is no new plans to stimulate production.

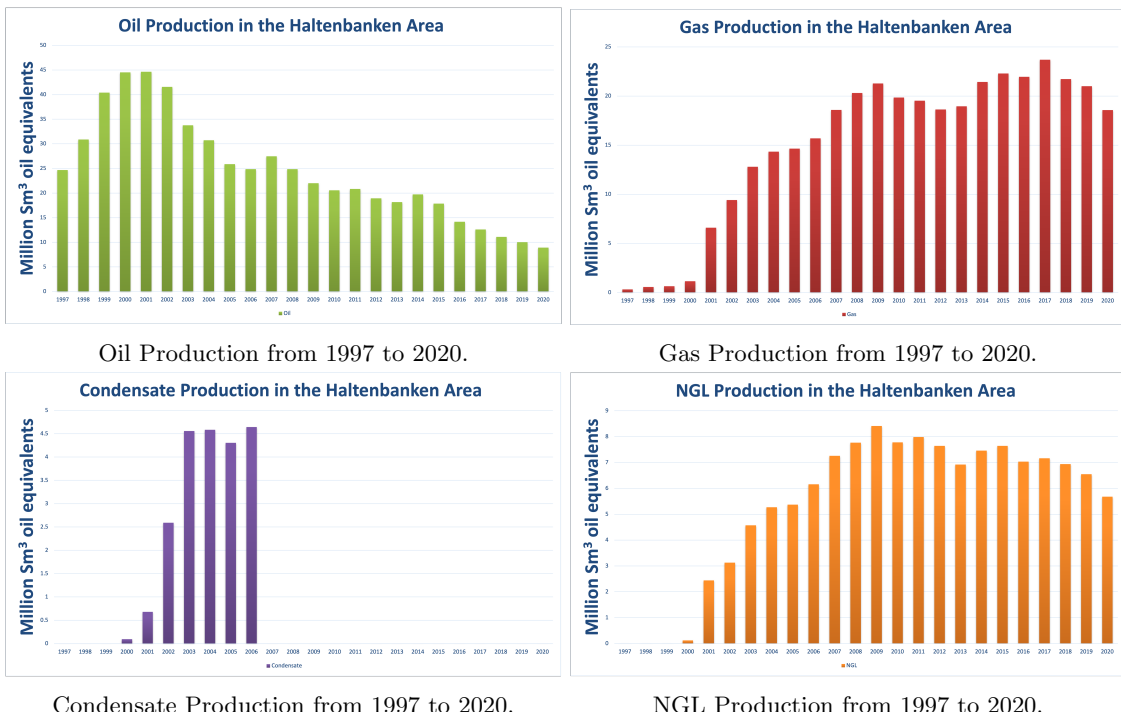


Figure 2: Oil, Gas, Condensate and NGL production in the Haltenbanken area from 1997 to 2020. All data are compiled from NPD website.

Source: [19]

## 2.4 CO<sub>2</sub> Emissions

Considering the total hydrocarbon production of these fields, given in Figure 3, we can see that there is a lot of activity and operations undergoing in the Haltenbanken area, which in turn produces CO<sub>2</sub>, which is released in the atmosphere. This CO<sub>2</sub> comes in two types of forms: direct emissions from the operational energy consumption of the oil rigs, vessels and subsea templates and indirect emissions from the burning of the gas and oil after it is transported to mainland. It can be used for industry, transport or in the consumer market.

Looking at the CO<sub>2</sub> emission history in the Haltenbanken area from 1997 to 2020 we can see that it has been slowly increasing until 2013, where there was a maximum of 2821 thousand tonnes of CO<sub>2</sub> produced, as shown in Figure 4. Since then, it has been slowly decreasing until 2020, when 2341 thousand tonnes of CO<sub>2</sub> were produced. This decrease is largely due to the fact that equipment efficiency has been improving (such as turbines), but also because of the digitalization and automation that has been undergoing in the last couple of years. Also, the total production has been decreasing over the last years.

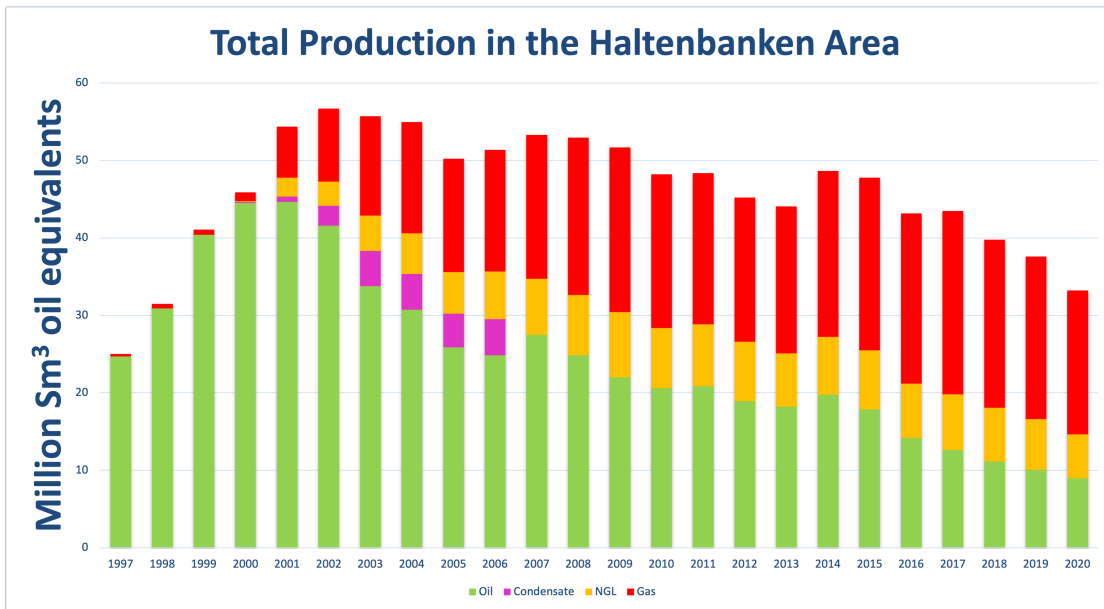


Figure 3: Total Production in the Haltenbanken area from 1997 to 2020 in Sm<sup>3</sup> oil equivalents. All data are compiled from NPD website.

Source: [19]

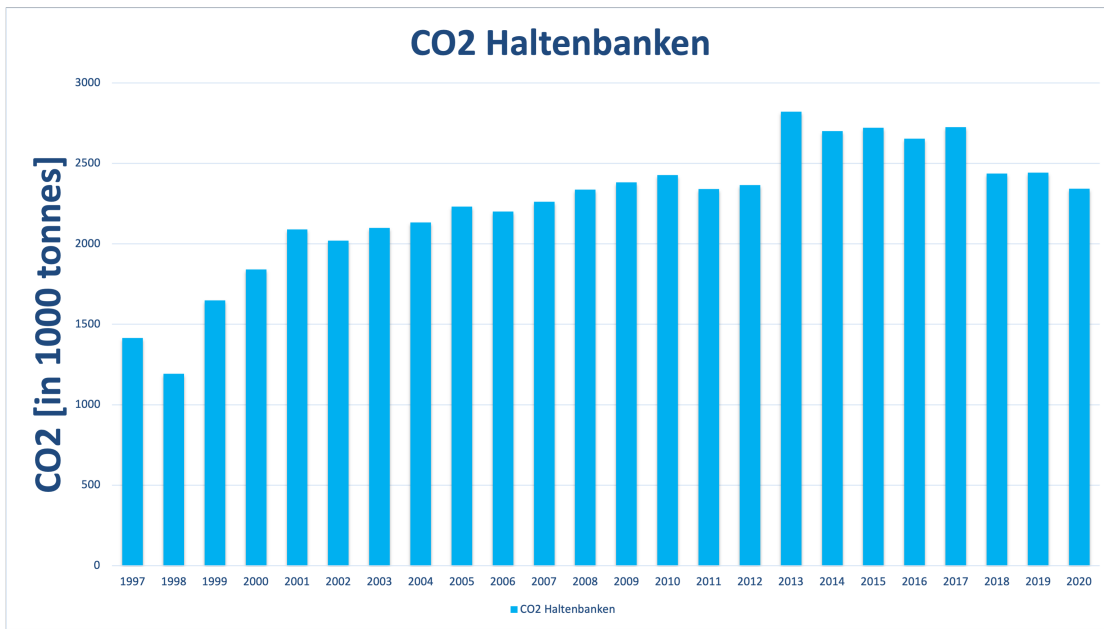


Figure 4: Total CO<sub>2</sub> emission in the Haltenbanken area from 1997 to 2020 in 1000 of tonnes. All data are compiled from NPD website.

Source: [19]

With the introduction of energy management systems and the installation of more energy-efficient equipment such as compressors and pumps, there has been a reduction in emissions related to petroleum activities. Looking at the main sources of direct emission of CO<sub>2</sub> we can see from Figure 5 that around 85% of all emissions come from the turbines. So, just by switching the energy provenance of the turbines, instead of using gas, the emission can be reduced drastically. This way, the industry can tackle the problem related to CO<sub>2</sub> emission that come with hydrocarbon extraction, but there is still a need to overcome the indirect emissions, that come when the hydrocarbons are utilized in the consumer market.

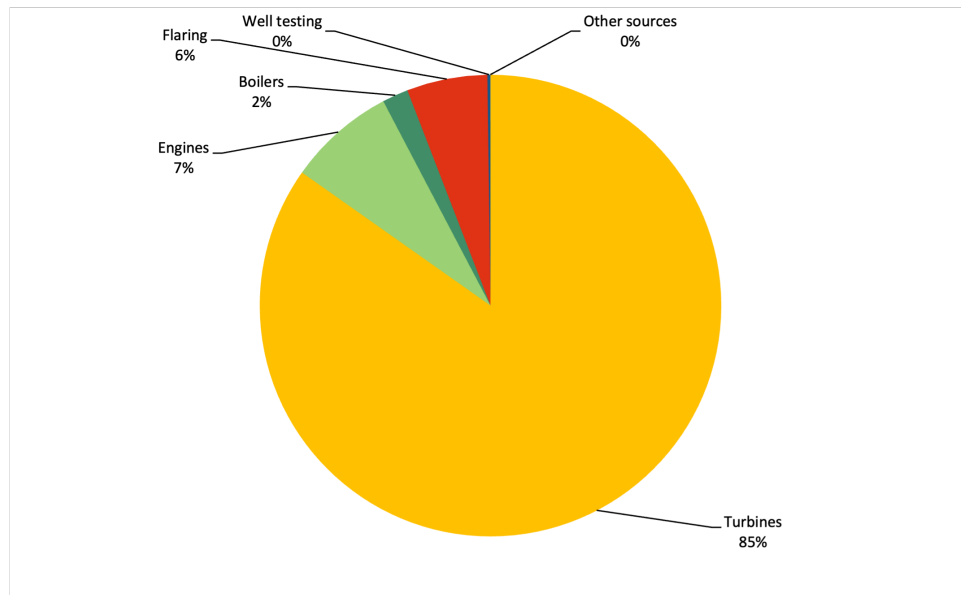


Figure 5: Total CO<sub>2</sub> emission in the Haltenbanken area from 1997 to 2020 in 1000 of tonnes. All data are compiled from NPD website.

Source: [19]

---

### 3 General Solution

This study is aimed towards 15 oil and gas fields located in the Haltenbanken area (that are being produced by several companies). Of these, 12 are operational at this moment, and 2 more will be back in production by the end of this year. One thing to consider is that the area has a well developed infrastructure, as seen in Figure 18 in Appendix A. There are rigs, vessels, subsea templates and a well defined network of pipelines. Moreover, there are many fields that are planned to be developed in the near future.

When talking about CO<sub>2</sub> reduction we will categorize the emission by provenance: direct emissions and indirect emissions, as discussed in Section 2.4. Pertaining to direct emissions, most of the energy used for oil and gas extraction comes from burning natural gas on the platforms in order to power all the operations. This, in turn, releases a large amount of CO<sub>2</sub> in the atmosphere, as we have seen in Figure 5. By switching, from burning natural gas, to a more environmentally efficient and non-polluting form of energy, we can drastically decrease the CO<sub>2</sub> footprint. One way of doing this is by using hydrogen as the main fuel. Hydrogen can also be sold to the consumer market. Thus, we can reduce both the direct and indirect CO<sub>2</sub> emissions.

This project revolves around the idea of producing hydrogen. In this solution we start by transforming a part of the natural gas that is being produced (30% off the total amount) into hydrogen by making use of gas reforming processes. This will be done in an offshore hub, which will be located between the Asgard and Heidrun fields. So, the hydrogen production plants will be located on offshore vessels. Some of the produced hydrogen will be used to power and offer the required energy for the operations on the rigs, vessels and subsea templates, while the rest of the hydrogen will be transported via a pipeline to the mainland where it will be sold to the consumer market. In order to power these hydrogen plants, a nearby offshore windmill farm will be established in order to produce clean, renewable energy for the hydrogen production.

Another thing to consider is that the transformation of natural gas into hydrogen will still yield CO<sub>2</sub> in the process as a byproduct. So, it is necessary to capture this CO<sub>2</sub> and store it in a suitable location, such as nearby saline aquifers (CCS) that are large enough to accommodate all the injected CO<sub>2</sub>. An illustration of the solution is given in Figure 6.

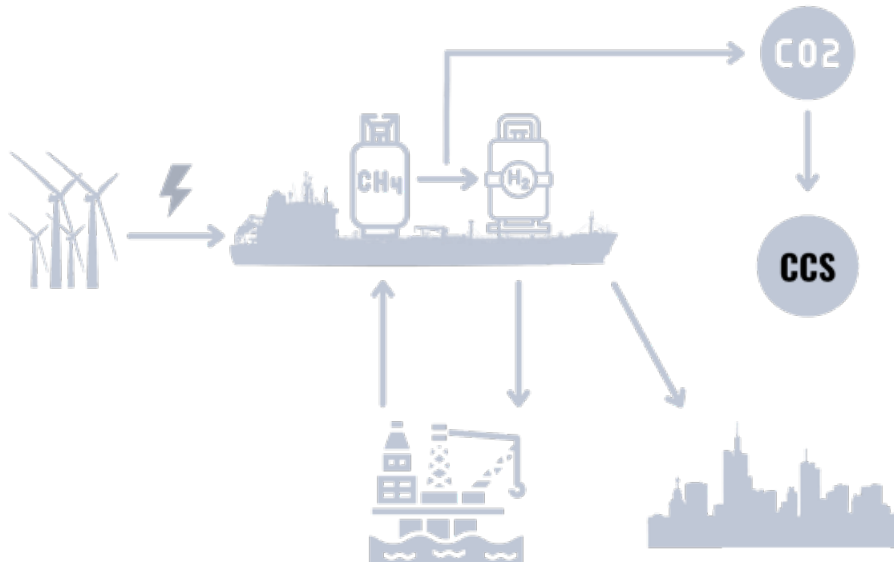


Figure 6: Illustration of the proposed solution.

---

The solution has many different components that need to be examined in more detail. Section 4 to 7 will go into more detail on the different components of the solution. This project also has the possibility to be upscaled in the future. As the hydrogen market becomes more mature, and the technology and infrastructure related to it develops, the total percentage of gas which is reformed to hydrogen can be increased.

## 4 Windmill Farm

A windmill farm will be established in order to produce renewable energy to the hydrogen production. It is estimated that the hydrogen production will need around 1650 GWh of energy per year based on the average gas production from 2015 to 2020, as shown in Table 1. The calculations for the required energy are further explained in Section 5.

Today bottom-fixed windmills are cheaper than offshore windmills. However, bottom-fixed windmills can only be installed at water depths up to 60 meters. In the Haltenbanken area the water depth is approximately around 250 to 350 meters, and offshore windmills are the only alternative. Offshore windmill farms are a new industry. The first full scale offshore windmill farm was opened by Equinor in 2017, called Hywind Scotland [20]. Equinor is also developing another offshore windmill farm called Hywind Tampen, that is due to start up in the third quarter of 2022. Hywind Tampen consists of 11 turbines with an 8 MW capacity each [21].

The offshore windmill industry is developing rapidly. New and better turbines are constantly being developed. It is therefore natural to believe that the capacity of these turbines will increase further in the upcoming years and be even more efficient. Today General Electrics have developed an offshore turbine called Haliade-X, with 14, 13 and 12 MW capacity. This is the most powerful offshore turbine built today [22]. So far there are only prototypes of the turbine operating, but there is only a matter of time before these turbines can be used commercially. With this taken into account we have chosen to calculate the energy using 12 MW turbines, as we believe this will be realistic for future projects.

It is estimated that the capacity factor of the turbines will be around 60%. This is higher than the ongoing Hywind Tampen project which has a 57.1% capacity factor [21]. However, the new Haliade-X turbines boasts of a capacity factor of 60-64% [22]. A capacity factor of 60% also seems reasonable according to [23], where the wind potential for Haltenbanken area has been analysed. Given a capacity factor of 60% and a 12 MW turbine, one windmill can generate 63 GWh of gross annual energy production. To meet the energy needs of the hydrogen production, at its peak, we will need 28 windmills, as shown in Table 1. This will give an expected yearly production of 1 764 GWh.

Year	Total natural gas [mill SM3]	30% hydrogen gas per day [MMSCFD]	Energy demand [GWh per year]	Windmills
2015	61.1	1709	1658	26.3
2016	60.1	1682	1632	25.9
2017	64.9	1815	1761	28.0
2018	59.5	1665	1616	25.7
2019	57.6	1610	1562	24.8
2020	50.7	1419	1377	21.9

Table 1: Energy demand for transformation of 30% of the natural gas to hydrogen.

### 4.1 Placement

The windmill farm will be situated close to the hydrogen production vessel, between Asgard and Heidrun. The placement is chosen to minimize the length of the submarine power cable between the windmill farm and the vessel. According to Equinor the Hywind Tampen project will take up an area of 21.9 km<sup>2</sup> for a windmill park of 11 windmills [21]. This corresponds to 55.75 km<sup>2</sup> for

this project. Taken into account that the windmills in this project are bigger it is assumed that the windmill farm will take up an area of approximately 60-80 km<sup>2</sup>. The distance between Heidrun and Åsgard is approximately 30 km, and it should be more than enough space for the windmill farm between the two platforms. It is assumed that the proposed windmill farm will not disturb the oil and gas production from the nearby fields.

## 4.2 Energy Storage

Offshore wind is a renewable energy source that gives variable energy supply that does not always match the consumer energy demand. This is a limiting factor to the windmill park as a supplier to the hydrogen production facilities. Hence, there is a need for energy storage at the production site. This energy storage will serve as a buffer to store excess energy at low demands and compensate for deficits at high demands. In doing so, the offshore wind will become a predictable clean energy source.

One promising concept to solve this problem is the FLASC technology. As conventional onshore energy storage technologies are not equally ideal for offshore applications, new technology might be needed. The device, that is FLASC, can be directly integrated with floating wind platforms. The energy is being stored using hydro-pneumatic liquid pistons which are driven by reversible pump-turbines. The concept works well for storage above 10MWh. For our project we estimate that a storage of 12MWh for each windmill will be suitable [24].

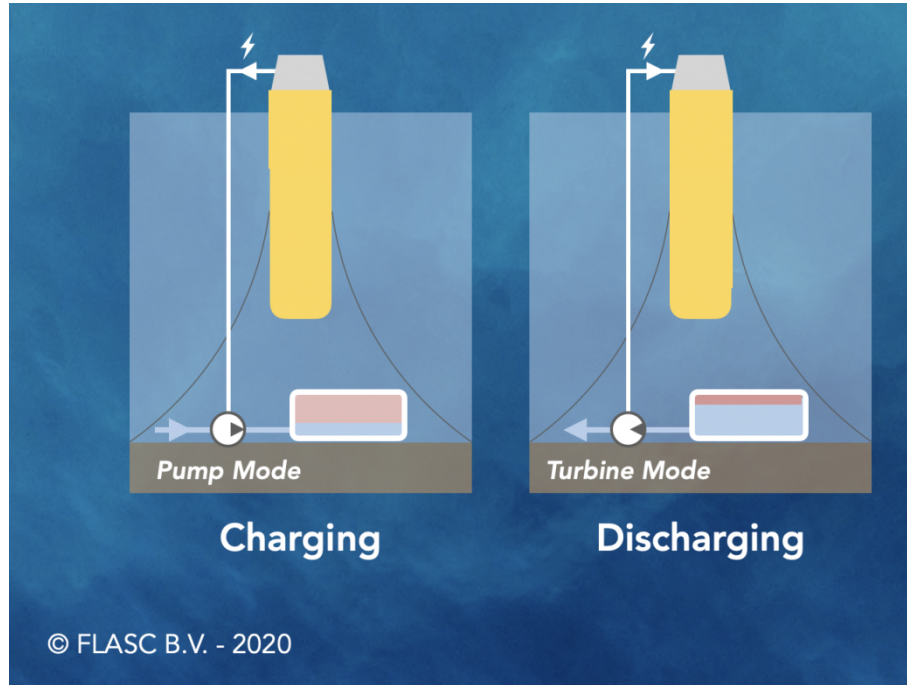


Figure 7: FLASC concept.

Source: [24]

As illustrated in Figure 7, in charging mode water is pumped into a closed chamber containing pre-charged air using electricity. At discharge, this pressurized water is released through a hydraulic turbine generating electricity.

---

## 5 Hydrogen Production

### 5.1 Methods

Due to some uncertainty as to which method of hydrogen production to base our solution on, two of the most common methods are reviewed. The methods are then compared and the most suited one is further described and adjusted to better match our proposed solution.

#### 5.1.1 Steam Methane Reforming

Steam methane reforming (SMR) is the most common way of producing hydrogen. It is a process where the methane contained in natural gas is used to produce hydrogen through thermal processes. It may be defined in the two stages of steam-methane reforming reaction and water-gas shift reaction. As methane enters the first stage from a natural gas source, it reacts with high temperature steam, typically at 700-1000 °C, pressurized at 3-25 bar [25]. In the presence of a catalyst it produces hydrogen, carbon monoxide and some carbon dioxide. It is an endothermic process that requires heat to be added, and the chemical reactions is as stated in Eqs. (1, 2).



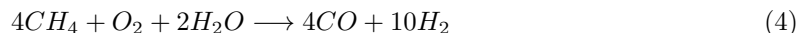
The next stage is the Water-gas shift (WGS) reaction, where carbon monoxide and steam are reacted using a catalyst to produce carbon dioxide and more hydrogen. The chemical reaction is as stated in Eq. (3).



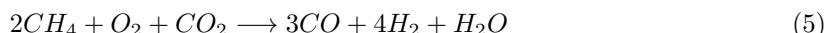
This is followed by a Pressure-swing adsorption (PSA), where most impurities are removed from the stream resulting in a high-purity hydrogen stream. The adsorbed components of the stream make up a high BTU fuel gas, normally transported back to the reformer to be fired for heat.

#### 5.1.2 Autothermal Reforming

Autothermal reforming (ATR) uses a preheated feedstock of natural gas to its reactor at 30-100 bar [26, 27]. First, the feed-gas reacts with oxygen and steam to produce syngas, a mixture of hydrogen and carbon monoxide. Then, in the same reactor, the gas mixture enters a catalyst bed for further reforming. It is an exothermic reaction and the chemical reaction is as stated in Eq. (4).



It is also possible to use carbon dioxide instead of steam. In this case, the reaction is described by Eq. (5).



The stream is finally cooled in a process gas boiler. This last step generates high-pressure steam which can be used for i.e. power generation. At last, the stream can be separated into pure hydrogen, carbon monoxide and carbon dioxide.

### 5.1.3 Comparison

The key difference between SMR and ATR is that SMR uses methane in reaction with steam, whereas ATR uses methane in reaction with oxygen and carbon dioxide or steam to form syngas [28]. Due to the nature of the reactions SMR is an endothermic process, as opposed to ATR which is an exothermic process [29]. In other words, SMR requires energy in form of heat to be added to the process, whereas ATR generates energy in form of heat. This excess energy might be used in other processes in the nearby area. Both devices use a catalyst in their processes and are the most common devices for methane reforming.

As can be noted from the reactions happening in the processes, SMR has the advantage of more hydrogen being produced from the same amount of methane. Although, this is dependent on the efficiency of the methane conversion. Another advantage of the SMR process is the possibility of being more cost-effective. Still, this depends on the size of the process plants and in what magnitude the excess energy from the ATR process is being utilized.

In conclusion, the group agrees that SMR looks to be the best fit and will be the simplest method for modification to include aspects that are essential in the realization of our solution.

## 5.2 Design

In designing the SMR process plant best serving our solution, some elements need to be integrated in the conventional SMR process. Namely, heat supply using energy from offshore wind, water treatment,  $\text{CO}_2$  removal, and impurity removal to ensure a high-purity end product. A Block flow diagram (BFD) showing a SMR process plant similar to our proposed solution is shown in Figure 8.

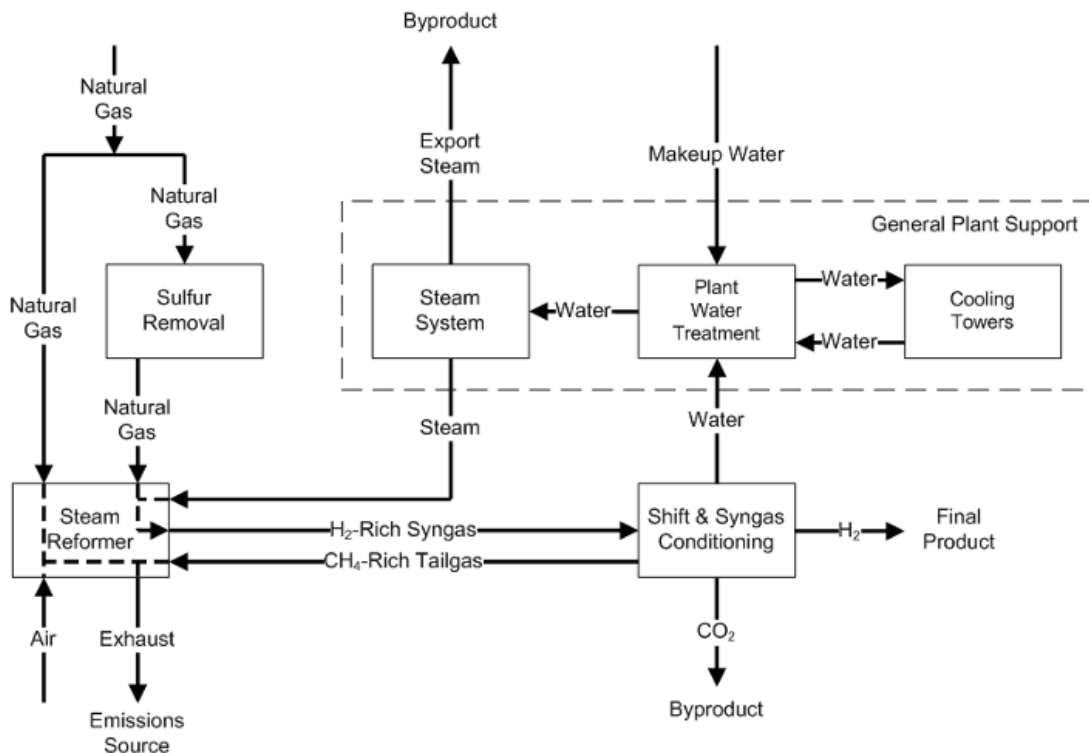


Figure 8: Block Flow Diagram of Conventional SMR Process Plant with Carbon Removal.

Source: [30]

The BFD shows two streams of natural gas entering the reformer, due to the fact that in conven-

tional SMR some amount of natural gas is burnt in the reformer for heat generation. Although, with heat being supplied solely from energy gained in the offshore wind farm, this second stream will not be needed. The temperature in the reformer is estimated to optimally be in the range 840-900 °C [30]. The stream is then run through heat exchangers at different stages through the rest of the process. This heat is used to supply the support plant.

Also entering the reformer is steam generated in the support plant. The stoichiometric water demand in the process is 4.5 L/kgH<sub>2</sub>, but in reality excess steam is needed for better operation. The actual water demand is therefore estimated to be 9 L/kgH<sub>2</sub> [31]. This is where a disadvantage arises, namely the fact that fresh water is needed in large proportion. Combined with the fact that the production is planned to be situated offshore, the easiest choice is thought to be using the surrounding sea water and desalinate it. Hence, a reverse osmosis plant is needed for the makeup water entering the support plant.

### 5.2.1 Carbon Removal

Few of today's conventional SMR process plants sequester the CO<sub>2</sub> removed from the stream. For our solution to be a better alternative than burning the natural gas directly, in terms of GHG-emissions, the CO<sub>2</sub> needs to be removed and captured. There are several options when it comes to CO<sub>2</sub> removal from the SMR process, but the deciding factors when choosing the best alternative will be the requirement of purity for the hydrogen product and the need to sequester the CO<sub>2</sub>. A good fit for our solution is high requirements for both these factors. A low risk solution is then to use well known technologies such as CO<sub>2</sub>-absorption for the CO<sub>2</sub> removal and PSA to ensure the purity of the hydrogen product [30].

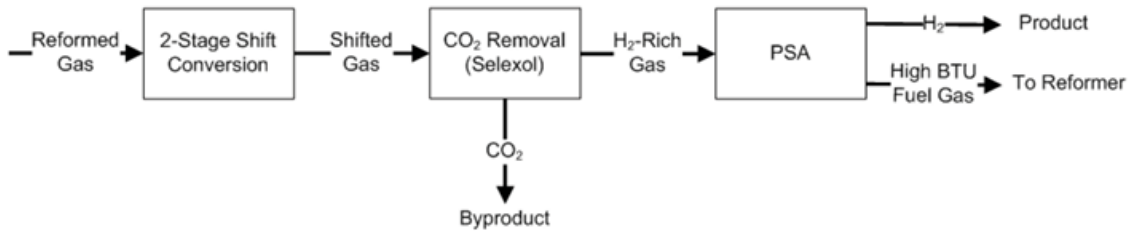


Figure 9: Block Flow Diagram of Shift & Syngas Conditioning.

Source: [30]

The proposed design of the Shift & Syngas Conditioning stages is shown in Figure 9. The syngas from the reformer enters a 2-stage shift conversion where CO is converted to CO<sub>2</sub> according to the reaction described in Eq. (3). In the first stage most of the CO is converted, as the reaction happens faster at elevated temperatures. The stream is then run through a heat exchanger to be cooled, lowering the CO equilibrium concentration, before entering the second WGS stage where most of the remaining CO is converted to CO<sub>2</sub>. In turn, hydrogen production is maximized.

As the shifted gas exits the WGS-stages, it is time to remove the CO<sub>2</sub>. The absorption is done using a commercial solvent, i.e. Selexol. The CO<sub>2</sub> is then captured and transported for further processing before being stored.

The last step remaining in this part of the process is to remove remaining impurities in the stream. This is done using PSA, as hydrogen is picked up in low amount using adsorption. Thus, an end product with purity of above 99% hydrogen is ensured. The removed components, namely CO, CO<sub>2</sub> and CH<sub>4</sub>, is then transported back to the reformer and fired to create heat used in the reformer reactions.

### 5.3 Calculations

Hydrogen and methane characteristics used in the calculations are listed in Tables 2 and 3. Parameters of the process plant is listed in Table 4.

	Hydrogen	Methane	Unit
Density (NTP)	0.08375	0.6680	[kg/m <sup>3</sup> ]
Gravimetric energy density	119.9600	50.0000	[MJ/kg]
Volumetric energy density	10.0467	33.4000	[MJ/m <sup>3</sup> ]
Specific energy	33.3222	13.8889	[kWh/kg]

Table 2: Characteristics - LHV.

	Hydrogen	Methane	Unit
Density (NTP)	0.08375	0.6680	[kg/m <sup>3</sup> ]
Gravimetric energy density	141.8000	55.5000	[MJ/kg]
Volumetric energy density	11.8758	37.0740	[MJ/m <sup>3</sup> ]
Specific energy	39.3889	15.4167	[kWh/kg]

Table 3: Characteristics - HHV.

Methane conversion ratio	0.78
Mass ratio ( $\frac{H_2}{CH_4}$ )	0.33
Volume ratio ( $\frac{H_2}{CH_4}$ )	2.64

Table 4: SMR parameters.

Calculations considering the SMR process were based on calculations done on a smaller plant, with layout as illustrated in Figure 8 [30]. A detailed description of values and parameters used in the calculations can be found in Appendix C. The result for the different streams and inputs of the process are listed in Table 5. The natural gas amount listed in the table is 30 % of an average extracted volume, calculated from extracted volumes from 2015 to 2020. From Table 5 one can calculate that the CO<sub>2</sub> absorption will capture 71%-72% of the CO<sub>2</sub>, and the annual amount of removed CO<sub>2</sub> will be 9.9 million tonnes. According to this an annual CCS capacity of approximately 10 million tonnes is required.

Stream	Value	Unit
Natural gas	17.70	[10 <sup>6</sup> ·m <sup>3</sup> /day]
Hydrogen	46.73	[10 <sup>6</sup> ·m <sup>3</sup> /day]
Water	3913.25	[m <sup>3</sup> /day]
CO <sub>2</sub> (removed)	27201.64	[tonnes/day]
CO <sub>2</sub> (emitted)	10852.73	[tonnes/day]

Table 5: SMR - Mass and volume flows.

#### 5.3.1 Energy Demand

In order to size the offshore wind farm needed to supply the SMR process plant, the energy demand needed to be calculated. The energy demand also make up the majority of the operational costs needed for the Economic analysis in Section 8. Table 6 lists how the daily energy consumption is distributed in the process plant. This result is based on the mass and volume flows listed in Table 6. It is worth to mention that the energy needed to supply the SMR process with fresh water by a reverse osmosis process is not included in these calculations, but it is estimated that it would account for approximately 60 % of the total energy demand [32].

Utility	MW	Percentage
NG reforming	41.89	22.92
Syngas purification	29.19	15.97
Steam system	2.54	1.39
CO <sub>2</sub> compression	90.12	49.31
Cooling towers	1.27	0.69
Water treatment	17.77	9.72
Total	182.78	100

Table 6: Daily energy demand.

### 5.3.2 Facility

It is estimated that the hydrogen facility need to have a capacity of 7.15GW. This has been estimated by scaling the capacity of the H21 project. The H21 project needed a capacity of 12.15 GW to produce hydrogen with an annual energy content of 85TWh [33]. In our project we will produce hydrogen equivalent to around 50 TWh per year. With a capacity of 7.15 GWh the facility must in average run at 80% in order to produce 50TWh.

In the project report of the H21-project, research was done on area requirements for land-based hydrogen production sites [33]. This was used as a base for decisions made on the facility vessel for our solution. In conclusion with village supervisor Nan Cheng of Equinor, an assumption was made on the possibility of using a down-scale factor of 5 when comparing land-based to offshore production. The H21-project estimate an area requirement of 0.9 km<sup>2</sup> for production facility of 12.15 GW capacity. Adjusted to our production capacity, this translates to an area requirement of 0.53 km<sup>2</sup>. Down-scaling this requirement for offshore production results in an area need of 0.106 km<sup>2</sup>. When comparing this area requirement to existing FPSOs, in the magnitude of the Skarv FPSO with LOA 295 m and width 50.6 m [34], a need for 8 production vessels is estimated. It is assumed that 90 % of the vessel area may be used for the process plant.

## 6 Carbon Capture and Storage

In our project we will capture CO<sub>2</sub> from the hydrogen reforming process explained in Section 5. The CO<sub>2</sub> will be transported in pipelines to storage sites and the CO<sub>2</sub> will be injected deep down in the ground in saline aquifers where it can be stored for thousands of years. The Carbon Capture and Storage (CCS) is a crucial part of this project. Without capturing the CO<sub>2</sub> emitted from the hydrogen transformation the emissions will be approximately the same as before.

For storing CO<sub>2</sub> we need to analyse the geology of the Haltenbanken area and investigate all the possible places for storing the CO<sub>2</sub> nearby. There are two different types of storage possibilities: either saline aquifers which are located in the Trøndelag platform or depleted oil and gas reservoirs in the Haltenbanken area. After investigating the different prospect the best location for drilling injections must be decided, considering capacity, costs, uncertainties and risks.

### 6.1 CCS in Norwegian Sea

To identify potential sites for CCS one must do geological assessments of the area. These assessments can vary from basin-scale studies to examination of the individual geological structures [35]. Some of the most important parameters when looking for potential storage sites are [36]:

- Permeability: The reservoir rock should be permeable to enable CO<sub>2</sub> migration from the injection point.
- Porosity: The rock should be porous so it can store large volume of CO<sub>2</sub>.

- 
- Volume: The thickness and area of the reservoir has to be sufficiently large, to provide large enough volumes available for storage.
  - Depth: The reservoir should be deeper than 800 m to be able to store CO<sub>2</sub> as a supercritical fluid. That is, a fluid that is neither liquid nor gas, but has some characteristics of both. However, the depth should not be too deep, as this is not economically feasible.
  - Seal: The reservoir should have a tight cap rock to prevent gas leakages to the surface.
  - Tectonic activity: The area should be stable without any significant earthquake activity.
  - Mineralogy: The reservoir should not contain any minerals that can deteriorate the quality of the reservoir during injection.

To assess information about the geology of the Norwegian Sea and information about the different aquifers the CO<sub>2</sub> Storage Atlas for the Norwegian Continental Shelf, published by NPD has been used [37]. The key information regarding the different aquifers are given in the following subsections.

In the southeastern part of the Norwegian Sea the groundwater aquifers have a slope of typically 1-2 degrees, from the Norwegian coast to the basin. Due to the slope and permeable substrates there is a risk of CO<sub>2</sub> migration upwards. It is important to understand the timing and extent of CO<sub>2</sub> migration when assessing the storage capacity of the aquifers [37].

The best general conditions which are met within the Trøndelag Platform pertain to the Jurassic succession, which is thick and contains several aquifers with good CO<sub>2</sub> storage potential.

Reservoirs that could possibly be used for CO<sub>2</sub> injection are Jurassic sandstones. The main sealing rocks in the area are the Melke Formation shales and the Middle to Upper Jurassic Spekk formations, as well as the fine-grained Cretaceous sandstone.

The main criteria for assessing CO<sub>2</sub> storage volume is to increase the acceptable pressure and limit CO<sub>2</sub> migration. CO<sub>2</sub> will move upwards as long as it has the possibility. To stop the migration the CO<sub>2</sub> must be permanently bound or trapped. This can be done by residually or structurally trapping the CO<sub>2</sub> or by letting the CO<sub>2</sub> diffuse within the formation water. Good CO<sub>2</sub> injection diffusion is vital to achieve sufficient volume trapping. When injecting the CO<sub>2</sub> we want to maximize horizontal surface expansions along the formation and minimize vertical expansions, to facilitate the CO<sub>2</sub> to dissolve in the formation water. To minimize vertical expansion CO<sub>2</sub> should be injected in the lower parts of the reservoir. The vertical expansions are dependent on the vertical permeability and the regional permeability distribution near the well. To maximize horizontal surface expansion, multiple injection wells should be used [37].

## 6.2 Aquifers

The Norwegian Sea shelf has several aquifers with good potential of CO<sub>2</sub> storage within the Trøndelag Platform: Åre/Tilje Aquifer, Ile/Garn Aquifer. These aquifers are located in the Jurassic succession. The Rogn formation is situated on the top of Ile/Garn aquifers, and could also be a good prospect for CO<sub>2</sub> storage [37]. From NGU report (no.2002.010) several wells in the Åre/Tilje and the Ile/Garn aquifers have been analysed [36]. The information in the following subsections are regained from the CO<sub>2</sub> storage atlas and the NGU report.

---

### 6.2.1 The Åre and Tilje

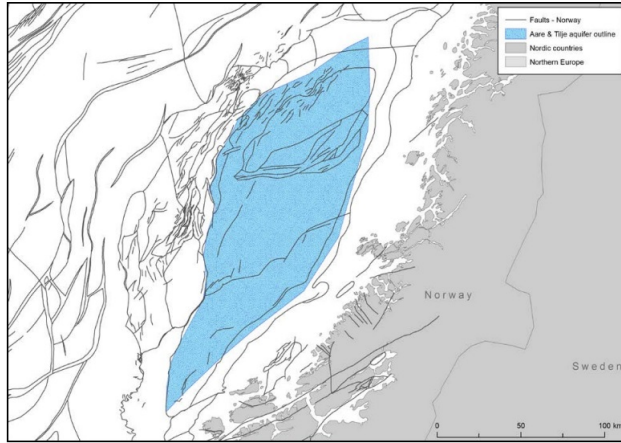


Figure 10: The Tijle/Åre aquifer

Source: [38]

As the name implies, this aquifer includes Tilje and Åre formation. Tilje formation consists of very fine to coarse-grained sandstones interbedded with shales and siltstones. Åre formation also has alternating sandstones and claystones interbedded with coals and coaly claystones. Due to the baffles and barriers, few related volumes are expected in Åre formation and also between the two formations. Due to this we might need several wells to inject the desired amount of CO<sub>2</sub>.

According to the well (6507/11-1) the Tilje formation occurs at 2596-2498 m depth with about 98 m thickness. The formation is uniformly developed throughout the Halten Terrace, where it is from 100 m to 150 m thick. In the northeast part it becomes thinner to less than 100 m on the Trøndelag Platform. The Tilje formation is overlain by Ror formation of the Båt group which is dominated by grey mudstones containing interbedded silty and sandy coarsening upward sequences, commonly a few meters thick. The Ror Formation varies from 70 m to 170 m in thickness. In several areas, the shaly formations of the Båt Group (Ror Formation) and the Fangst Group (group of several formations) may not act as good cap rocks. However, the overlying, 1000 m thick shale succession of the Viking Group is most probably tight [36].

Regarding the well (6507/12-1), the Åre formation occurs in depth 2929-2412 m and the thickness of the formation is about 508 m. The Åre formation has sand channels in shallow depth with good reservoir quality, however this potential decreases rapidly by increasing depth. It is estimated that the Åre Formation consists of approximately 30 % sandstone and 70 % claystones, coals and coaly claystones. The Åre Formation is overlain by the 100-150 m thick Tilje Formation which consists of sandstone interbedded with shale and siltstone [36].

The lower Åre-Tilje aquifer is distributed throughout the area and the potential injection volume is estimated at around 4Gt. The reservoir is heterogeneous, dominated by fluvial-deltaic to tidal deposits, and the connection of both local and regional scales is unclear [37].

The Åre/Tilje aquifer will probably have several internal cavities and barriers and this is considered as a closed aquifer [37]. A closed or confined aquifer is bounded with impervious or semi-impervious layers which cause pressure limitation for injecting CO<sub>2</sub> [39]. A table summarising the properties of the Åre/Tilje aquifer is given in Appendix D.

---

### 6.2.2 The Ile and Garn

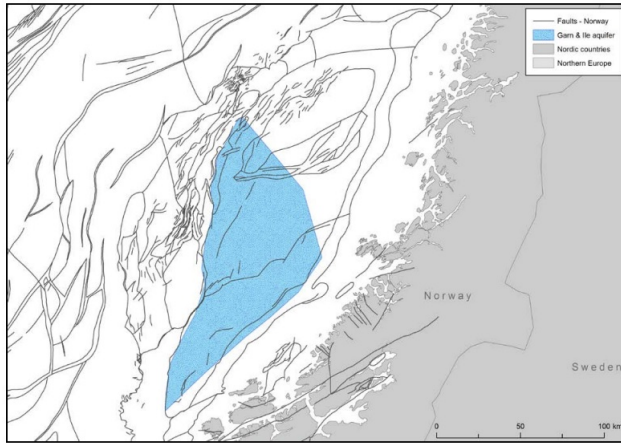


Figure 11: The Ile/Garn Aquifer

Source: [38]

The Ile and Garn formations have notable reservoir properties with higher porosity and permeability in comparison with the Tilje and Åre formations which are tidal dominated. Within the Froan Basin located in the southeastern part of the aquifers, the Garn formation is dominated by shallow marine sediments where a better connectivity can be expected. The shale in the Garn and Ile formations is increasing when moving towards the Helgeland basin. The Ile and Garn aquifers have a high potential to be used as a reservoir in the southeastern part of the aquifers, called the Froan Basin [37].

From well (6507/11-3), the Ile formation occurs in depth 2471.5-2536 m and the thickness is about 64.5 m. The top seal in the Ile formation is the Not Formation which consists of claystones and micronodular pyrite. From the NGU report the porosity of the sandstones in the Ile formation ranges from 17% to 30%. The Ile formation is a good candidate for storing CO<sub>2</sub>, due to the depth, top seal, porosity, permeability and mineralogy of the formation [36].

Based on the results from reference well (6401/1-3), the Garn formation occurs in depth of 3600 - 3704 m and the thickness is approximately 104 m. It is estimated that the formation consists of 90% sandstones and 10% shales. The formation is overlain by the Viking Group, which is the best seal for CO<sub>2</sub> storage due to shales and mudstones. The permeability and the porosity in the formation decreases with depth. The porosity varies from approximately 8-17% to 30%. The upper parts of the formations is therefore the best for injecting CO<sub>2</sub> [36]. A table summarising the properties of the Ile/Garn aquifer is given in Appendix D.

### 6.3 The Rogn formation

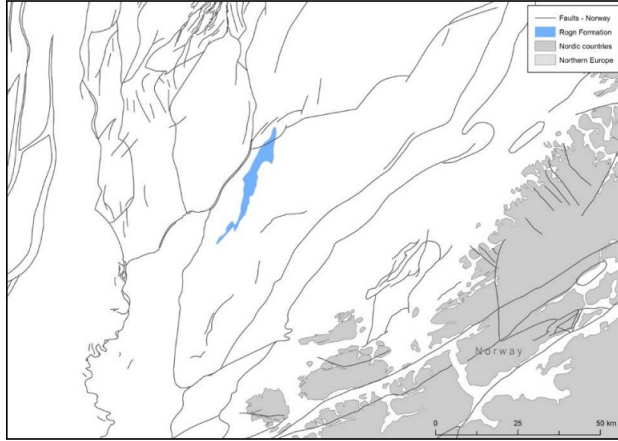


Figure 12: The late Jurassic Rogn Formation.

Source: [38]

The Rogn Fromation exists in several separate areas east of the Haltenbanken area. Regarding the well (6407/9-1) this formation occurs at depth 1621-1670 m, with a thickness of 49 m. The formation consists of 80% sandstone and 20% shales. The top seal of the Rogn Formation consists of shales from the Spekk formation, which is a good cap rock for storage. The Rogn Formation has very good reservoir characteristics. There are shales in the Spekk formation with different thicknesses between the Garn and Rogn formations, which separates them. It is expected that there will be connections between the Garn and Rogn formations. This means that if we inject CO<sub>2</sub> in the Garn formation some of it will migrate to the Rogn formation [36].

### 6.4 Depleted Reservoirs

Depleted reservoirs can be an important candidate for CO<sub>2</sub> storage. Two candidates to use for CO<sub>2</sub> storage for our project can be the Yttergryta reservoir and the Ormen Lange Reservoir. One advantage with Yttergryta is that it is at a closer distance from the hydrogen vessel, meaning a shorter transportation of the CO<sub>2</sub>. The placement is shown in Figure 1. The Ormen Lange field is situated southwest of the Haltenbanken area, further away from the vessel. Even though Ormen Lange is further away, it has good storage properties [37]. The reservoirs have a notable potential capacity. However, there are several challenges for reusing depleted oil and gas reservoirs for CCS. When the reservoirs are depleted the risk of pore collapse increases, which gives a loss of capacity and injectivity. Mechanical failure due to a weaken caprock, bounding faults or well completions can cause possible containment loss. Because of several existing wells in the reservoirs the risk of CO<sub>2</sub> leakage from well paths will increase. To prevent leakage the well paths must be sealed, which will give an extra cost. Reservoir fracturing can occur when injecting CO<sub>2</sub> in a dense phase, because of the low pressure in the reservoir [40]. Due to these risks we have decided to focus on saline aquifers in this project.

### 6.5 Decision

After reviewing the possible aquifers and depleted reservoirs we have decided to choose the Ile/Garn aquifer as our storage. The Ile/Garn aquifer had the best properties for CO<sub>2</sub> storing. The aquifer had high porosity, high permeability and a higher fraction of sandstone. The Not formation as a seal for the Ile formation and the Viking group as a seal for the Garn formation consists of shale and claystones which will make them good caprocks. Because of the decreasing porosity and permeability by depth in the Garn formation the CO<sub>2</sub> should be injected at the upper part of the

---

formation. The Rogn Formation is connected to the aquifer in some parts. This means that if we inject CO<sub>2</sub> in the Garn formation some of it will migrate to the Rogn formation and the capacity will increase.

A simulation were CO<sub>2</sub> was injected in the Ile/Garn aquifer from the Froan basin has been done by the NPD in the CO<sub>2</sub> storage Atlas [37]. The results from this simulation showed that about 400 million tons of CO<sub>2</sub> can be stored in the Garn and Ile aquifers. After 10 thousand years most of the gas will have dissolved with the water of the formation or be trapped [37]. Based on the information available we recommend the injection wells for the aquifer to be placed in the area of the Froan Basin, as it has the best potential for CO<sub>2</sub> storage. The simulations mentioned above has also been conducted with regards to the Froan Basin, which means that we have more data from this area.

## 6.6 Well design

The information from the NGU report (no.2002.010) [36] have been used for calculating the injection rate and considering our target CO<sub>2</sub> injection volume of 10 Mtpa. The following equation have been used to calculate the injection rate,  $q_{\bar{o}}$ , in excel:

$$q_{\bar{o}} = \frac{k_H \cdot h}{18.68 \cdot (\mu_0 \cdot B_0)_{@p_{av}} \cdot [\ln(\frac{r_e}{r_w}) - 0.75 + s + s_A]} [p_b - p_r] \quad (6)$$

The parameters used in Eq. (6) is given in Table 13 in Appendix D. The results from the calculations are also given in Appendix D in Table 14. The summary of the calculations are given in Table 7 below.

Summary		
Reservoir Pressure	Bar	204
Fracture Pressure	Bar	329
Fracture Pressure with Safety Margin	Bar	313
Max. Wellhead Pressure, Pwh	Bar	243
Bottom hole Pressure, Pbh	Bar	313
Injection Rate	Ton/year	2754985
Number of Wells Required		4

Table 7: The summary of well design.

## 6.7 Monitoring plan

CCS is considered a safe and reliable option for mitigating the increasing levels of CO<sub>2</sub> in the atmosphere. To assure safe CO<sub>2</sub> storage and minimize the risk of leakage, optimize injection operations, and confirm the storage volumes, it is necessary to propose short and long term monitoring plans [41].

The MMV programme, as the short form of measurement, monitoring and verification for CO<sub>2</sub> storage, is divided into the following project phases [42]:

- Pre-injection
- Operational
- Site closure
- Post-closure

Measuring wellhead pressure and temperature is the most widely used monitoring system that can be done for this project using sensitive acoustic sensors and electronics to observe any abnormal

---

changes, which will lead to taking actions upon that. The presence of this monitoring system is vital as the active injected well is associated with the highest possibility of leakage and release of CO<sub>2</sub> into the sea [43]. Moreover, PDGs (Permanent Downhole Gauge) tools can be used in order to detect the development and potential anomalies in injectivity [42]. Downhole fluid sampling can be done every year to enable the chemical analyses on the fluid in the reservoir to measure the fluid saturation changes.

Measurements at the wellhead or in the downhole can be done continuously and have a relatively low cost. But, the information we get from these methods is not enough for us to have a good overview during a long time monitoring program. This is why we need to use other more expensive tools.

Despite the high expenses due to conducting repeated 3D seismic surveys, they are the most efficient tool to control the project monitoring. By acquiring 3D seismic at different times over the injection area we can detect the CO<sub>2</sub> plume movement. Also, from this we can derive saturation and pressure changes over time, which allows us to better observe the distribution of the injected CO<sub>2</sub>. Over time, the repeat interval between 3D seismic surveys can be longer, however for the first years of injection, it is better to repeat the seismic surveys more frequently.

Also, time-lapse gravity field monitoring has been proven to be accurate for offshore projects to aid the assurance of the mass balance of the projects and estimating the mean of CO<sub>2</sub> density at reservoir conditions [42].

Pertaining to our project, we propose that we have one 3D seismic survey before any injection operation starts, in order to serve as a baseline for subsequent repeated surveys. Six seismic surveys can be done during the operation period. The repeat interval between each survey gradually increases since they are costly. As time goes by, the safety of the project increases. Lastly, only three gravity surveys need to be conducted due to the costs of this monitoring tool. Our proposed monitoring plan is illustrated in Table 8.

	Pre Injection	Operation										Post Injection
		+0	+2	+4	+6	+8	+10	+12	+14	+16	+18	
Monitoring plan	+0	✓	✓	✓	✓		✓		✓		✓	+20
Repeated 3D-Seismic		✓					✓			✓		✓
Time-Laps Gravity			✓			✓			✓			
Wellhead Pressure	✓	✓	✓	✓	✓	✓	✓	✓	✓	✓	✓	✓
Downhole gauges	✓	✓	✓	✓	✓	✓	✓	✓	✓	✓	✓	✓
Downhole Fluid Sampling	✓	✓	✓	✓	✓	✓	✓	✓	✓	✓	✓	✓

Table 8: Summary of the proposed monitoring plan.

## 7 Transportation

### 7.1 Hydrogen Transportation

A part of the hydrogen should be used as energy on the oil and gas platforms, while the rest will be transported to mainland. There are essentially two possible ways to transport the hydrogen. Either by ships or by pipelines. If ships are used the hydrogen must either be compressed into liquid state or transformed into ammonia for easier handling and distribution. By using liquid hydrogen or ammonia another process must be implemented in the hydrogen production facility.

By using pipelines it is not necessary to transform the hydrogen gas. However, installing new pipelines requires a big cost. High initial capital cost of new pipeline construction is a major barrier to expand hydrogen pipeline infrastructure [44]. Nevertheless, pipelines were regarded as the most promising concept for our project.

For this project we looked into the possibility to use existing gas pipelines to transport the hydrogen to mainland. One promising idea was to use the existing Haltenpipe to transport hydrogen. However, the capacity of the existing Haltenpipe is 7 million Sm<sup>3</sup> per day, which was to low for the estimated amount of hydrogen gas [45]. It is possible to convert natural gas pipelines to transport pure hydrogen, but this require a substantial modification. Another solution could be to convert existing natural gas pipelines to transport a blend of natural gas and hydrogen (up to 15% hydrogen) with only modest modifications on the pipeline [46]. Even though it will not be used in this project, we believe that converting gas pipeline to hydrogen pipelines could be an innovative solution and very relevant for future projects. Today there is an ongoing research project called HyLINE at SINTEF in collaboration with NTNU to investigate the possible to transport hydrogen in the existing subsea pipeline network in Norway [47].

In this project a new pipeline will be built next to the existing Haltenpipe, as the existing pipe didn't have the desired capacity. The new pipe will go from Heidrun to Tjelbergodden to transport hydrogen to the mainland. Hydrogen must also be transported back to the oil and gas platforms where they will burn it to produce energy. The platforms that will receive hydrogen is Norne, Skarv, Heidrun, Åsgard, Kristin, Draugen and Njord. For the two platform furthest north, Norne and Skarv, a new hydrogen pipeline must be installed. For the other platforms there will be established new pipelines from outtakes from the new "Haltenpipe" to the platforms. An illustration of the infrastructure of the hydrogen pipelines are given in Figure 13. For estimating the length of the pipelines the distances between the platforms have been measured and 10% of the length have been added. For example is the distance between Heidrun and Åsgard 36 km and the pipeline is estimated to  $36 \text{ km} \cdot 1.10 = 39.6 \text{ km}$ . This is chosen after comparing the length of the existing gas pipelines to the distance between the platforms. The estimated lengths are shown in Table 9.

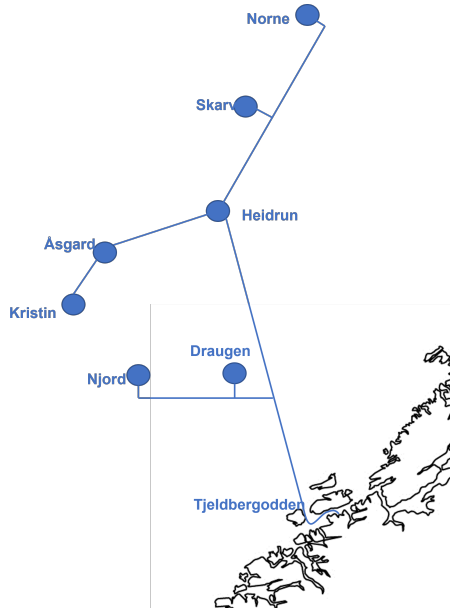


Figure 13: Illustration of the proposed hydrogen pipeline network. The distances in the illustration are not to scale.

	Distance [km]	Type
Haltenpipe: Heidrun - Tjelbergodden	250	New hydrogen pipeline
Haltenpipe - Draugen	11.0	New hydrogen pipeline
Draugen - Njord	29.7	New hydrogen pipeline
Heidrun - Åsgard	39.6	New hydrogen pipeline
Åsgard - Kristin	17.6	New hydrogen pipeline
Heidrun - Skarv	48.4	New hydrogen pipeline
Skarv - Norne	46.2	New hydrogen pipeline
Total	443	

Table 9: Estimated length of hydrogen transport pipeline network. Measured distances is taken from maps from NPD.

Source: [48]

## 7.2 CO<sub>2</sub> transportation

A vital component of a CCS scheme that is always overlooked is the transportation system. Carbon dioxide can be transported between capture points and storage sites by pipe, road tanker or ship. Since our CO<sub>2</sub> capture is done in an offshore hub and our CCS storage site is offshore as well, we need to choose the most efficient transportation option between ships and offshore pipelines.

In the case of transportation of CO<sub>2</sub> by ship, the CO<sub>2</sub> is compressed to be held just above the boiling line (Table 10), with smaller shipping solutions opting for higher pressure and higher temperature (e.g. around - 20 °C and 20 bar for ships of around 1000–2000 tonnes). But for larger scale shipping with larger tanks, the pressure needs to be reduced, requiring chilling the CO<sub>2</sub> to around -45 °C. The CO<sub>2</sub> will then need further compression at the storage site to reach the required injection wellhead pressure [49].

Regarding transportation of CO<sub>2</sub> by pipeline, the carbon dioxide is transported in the dense or supercritical phase. Operating in this regime reduces viscosity and surface tension while increasing density. Therefore, this is the most efficient way of transporting carbon dioxide; also, this phase transition leads to very effective use of the pore space as CO<sub>2</sub> in the subsurface occupies a much smaller volume than at the surface.

Properties	Units	Typical LNG	Typical CO <sub>2</sub> Transport by ship	Typical CO <sub>2</sub> Transport by pipeline
Fluid		Liquid	Semi-refrigerated liquid	Semi-refrigerated liquid (Dense phase)
Density	Kg/m <sup>3</sup>	450	1163	338
Density ratio (Gas/Liquid)		600	563	424
Pressure (gauge)	MPa	0.005	0.65	7.3-15
Temperature	K	113	221	293

Table 10: Typical conditions and properties across the shipping chain and pipeline. Data are compiled from the source.

Source: [49]

Considering the cost versus distance graph for CO<sub>2</sub> transportation by pipeline and ship, as seen in Figure 14, we can see that ships are most suitable for long distances, but smaller CO<sub>2</sub> volumes. While, pipelines are more cost effective when we are dealing with smaller distance, but large volumes. Also, while the CAPEX cost is higher with pipelines, the OPEX costs are much lower.

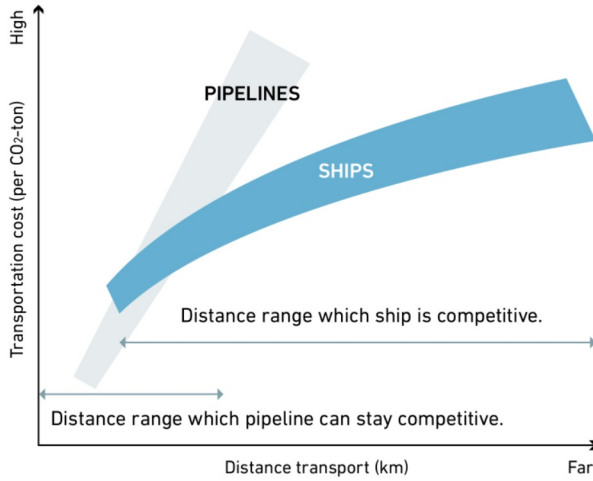


Figure 14: Transportation cost comparison - "Ship vs Pipeline".

Source: [50]

Looking at the distances in our project has proven helpful in identifying the pipeline as the leading transportation solution for our CO<sub>2</sub> project, as illustrated in Figure 15. Transport of CO<sub>2</sub> for sequestration requires a coordinated and efficient transportation network and pipelines are the most obvious solution, particularly where a constant flow from the CO<sub>2</sub> capture sites is required. Also, as we are dealing with a large scale project, the use of pipelines is justified as the transportation method. Pipelines show better performance than shipping with regards to fuel, electricity, and water consumption in the chain, generating a transportation system with an overall lower greenhouse gas emission footprint.

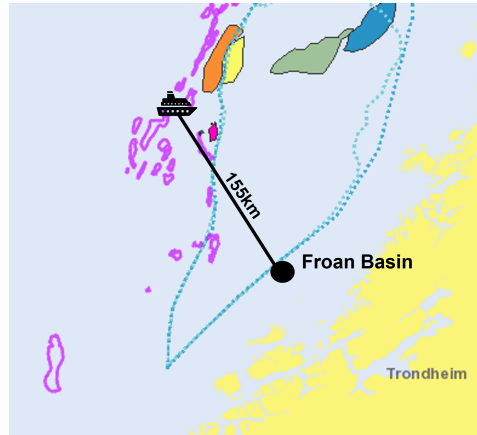


Figure 15: Distance between our Capture Point and the injection site.

Source: [48]

## 8 Economy

This project is a new and innovative project, based on several up and coming new technologies. Because of this there are big uncertainties when it comes to projecting the cost of the project. Some of the technologies used in the project is under development or still on prototype level, making it hard to find exact costs for the products. The results given in this section must therefore be considered as a rough estimate of the finances in the project. In the calculations a discount rate of 10% is used. The net present value of the project is calculated, assuming a lifetime of 20 years

without any major modifications or upgrades.

The estimated Capital Expenditure (CAPEX) and Operational Expenditure (OPEX) of the project has been estimated. The results are given in Table 15 in Appendix E. The distribution of the costs for the different aspects of the project is illustrated in Figure 16. The estimated CAPEX and OPEX of the project are given in Table 15. The distribution of the costs for the different aspects of the project is illustrated in Figure 16. One can see that for the CAPEX the hydrogen facility and the CCS will be the main contributors. For the OPEX however, the windmill farm is the main contributor. It is assumed that the OPEX of the windmill farm will be 30% of the CAPEX for the windmill farm [51]. However, this number can be discussed as new research show that it can be lower [52]. An extra margin of 10% has been added for the costs, to include uncertainties and unforeseen expenses.

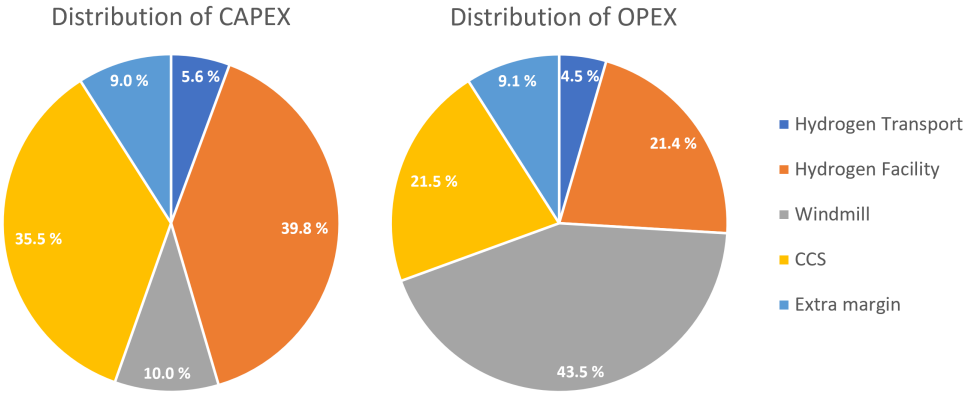


Figure 16: Distribution of CAPEX and OPEX in the project.

Figure 17 shows the development of the calculated Net Present Value (NPV) for the project, given that it started in 2022. It is assumed that the project will have a lifetime of 20 years before any major modifications or upgrades must be done. Based on the estimations the project will break even in 2031 and have a total profit of 82 billion NOK over the 20 years. A NPV above zero suggests that the project will be profitable. However, there are several factors and costs that have not been taken into account that can influence the NPV. Some of the costs that has not been included is costs regarding consulting services, costs for compressors in the pipeline system and operational costs for manpower and people working with the project. The NPV of the project is highly sensitive with regard to the hydrogen price. In this analysis the hydrogen price is set to be 3 \$/kg, but a small change to this value will have a great impact on the NPV and the feasibility of the project. Due to this a value in the lower area was chosen, to avoid an overestimate of the income.

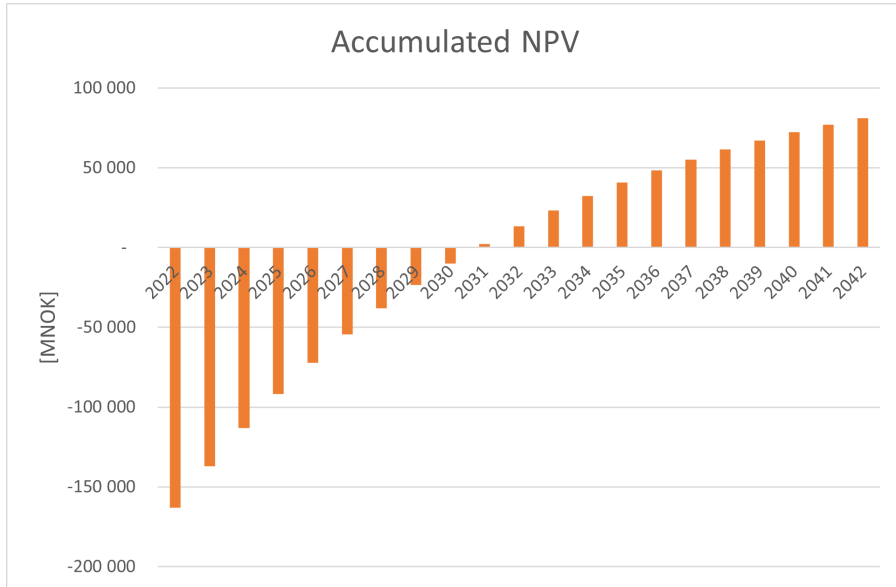


Figure 17: Development of NPV throughout a lifetime of 20 years.

In the following subsections the calculated cost estimates are further explained. In Appendix E an overview of all the calculations are given.

## 8.1 Windmill Farm

The calculations of the cost of the offshore windmill farm are based upon the costs of the Hywind Scotland project and the assumed costs of the Hywind Tampen project. Equinor has stated that they expect drop of 40% for CAPEX/MW between the two projects [53]. The Hywind Scotland project had a CAPEX of £264 mill for 30MW capacity, which gives £8.8 mill/MW, equivalent to approximately 113 MNOK/MW [54]. The Hywind Tampen project is assumed to cost 5000 MNOK for a 88MW capacity facility, equivalent to 56.8 MNOK/MW [55]. If the Hywind Tampen project adheres to the budget this will give a reduction of CAPEX/MW of around 50%. Equinor expect a further reduction of 25% in CAPEX/MW for the next project with a capacity around 200MW [56]. Using these numbers we get an expected cost of 24.61 MNOK/MW for the windmill farm. With an installed capacity of  $28 \times 12\text{MW} = 336\text{MW}$  this will give a total CAPEX of 14 318 MNOK for the windmills. The OPEX of the windmills are estimated to be 30% of the CAPEX in accordance to [51]. For the power cable a unit price of £2.5 mill/km has been used for calculating the CAPEX, while it is assumed that the OPEX will be 6% of the CAPEX price [57].

For the energy storage the price has been estimated based on prices for batteries containing the same amount of energy. It was assumed a price of 300\$/kWh (2020), giving a total CAPEX of 853 MNOK. The OPEX was estimated to be 10% of the CAPEX [58].

## 8.2 Hydrogen Production

The hydrogen production facility will have a capacity of 7.15GW in order to transform 30% of the natural gas. To estimate the costs of such a facility we have compared with the H21 North of England project. In this project they estimate the price of a 12.15GW natural gas-based hydrogen production facility to have a CAPEX of £8 520 million and an OPEX of £285 million [33]. Scaling this to our facility we get a CAPEX of £5 014 million and an OPEX of £168 million. The cost of the electricity to power the facility is excluded, as this has been taken into account by the costs of the windmill farm. One significant difference from the H21 Hydrogen facility is that the facility in this project will be situated on vessels. It is assumed that the costs for chartering vessels will be

---

\$27 500/day per vessel, given in 2016 \$, for the first 10 years. After this the cost will be reduced to 50% for year 11 to 15 and 30% of the original cost for year 16 to 20 [59].

### **Hydrogen Transportation**

According to H2A delivery model also called HDSAM (Hydrogen Delivery Scenario Analysis Model) produced for the U.S Department of Energy at Argonne National Laboratory (ANL) the cost of a hydrogen pipeline is 10% higher than an equivalent gas pipeline [60]. This model is valid for onshore pipeline, but it is assumed that the same factor can be used for subsea pipelines, since the additional cost of the hydrogen pipeline is associated with increased production costs. From the village an estimate of 15-19 million NOK/km was given for gas pipelines. Using the the upper limit of this with a factor of 1.1 gives an estimate of 20.9 million NOK/km for the hydrogen pipelines.

## **8.3 CCS**

The cost estimate for capturing the CO<sub>2</sub> is included in the cost estimate for the hydrogen facility. For storing the CO<sub>2</sub> the report "Potential for reduced costs for carbon capture, transport and storage value chains (CCS)" from DNV GL Energy has been used. The report stated that CAPEX for storing 0.8 Mtpa was 5 575 MNOK and the OPEX 167 MNOK in 2018 NOK [61]. These numbers have been scaled to our project to get an estimate of the costs. For transporting the CO<sub>2</sub> the cost of the pipelines have been estimated to 19MNOK/km, based on numbers given in the EiT village. It has been estimated that the total length of the pipelines will not exceed 180 km. The OPEX costs of the pipelines have been estimated from the article [62] by using exponential interpolation for storage capacity between 2.5 and 20 Mtpa. For this project a storage capacity of 8 to 10 Mtpa is used.

## **8.4 Income**

The project's main income will come from selling the excess hydrogen to mainland. Additionally there will be an income source in terms of saved expenses from CO<sub>2</sub> quotas. There could also be possibilities for the project to get financial support from the government, since it is a new and innovative project that would contribute to reducing CO<sub>2</sub> emissions. However, this has not been taken into account when calculating the income.

### **Hydrogen sale**

It is estimated that the Haltenbanken area will require around 10% of the produced hydrogen to meet the energy demand. The rest of the hydrogen will be transported to mainland and sold. 90% of the hydrogen is estimated to be 1286 million kg, looking at the average gas production for the last 5 years. Given an assumed hydrogen price of 3 €/kg based on [63], the estimated income will be 37 billion NOK per year.

### **Saved expenses CO<sub>2</sub> quotas**

As of the 18th of April 2022 the EU ETS carbon price is €80 /tonnes [64]. For the period 2015 to 2020, the Haltenbanken area released in average 2 500 000 tonnes CO<sub>2</sub> from burning natural gas to get electrical power per year. The hydrogen facility will capture around 71% of the CO<sub>2</sub> produced in the facility. With today's carbon price this corresponds to €1 380 million NOK per year in saved expenses for the Haltenbanken area from CO<sub>2</sub> quotas if the project is implemented. The Norwegian government has stated that they will increase the tax price on CO<sub>2</sub> quotas to 2000 NOK/tonnes in 2030 [65]. Due to this the expected saved expenses will increase in the upcoming years. However, as a conservative assumption we have decided to use a fixed price of €80 /tonnes in our calculations.

## **9 Conclusion**

The project will reduce both direct and indirect CO<sub>2</sub> emissions in the Haltenbanken area. 71-72% of the CO<sub>2</sub> from hydrogen transformation process will be captured. This will reduce the total

---

emission with approximately 10 million tonnes of CO<sub>2</sub> each year. 10% of the reduced emissions will be saved direct emissions while 90% of the emissions will be saved indirect emissions. The direct emissions which are reduced comes from the implementation of burning hydrogen instead of natural gas on the platforms to produce energy.

This project is based on several up and coming new technologies. Many of these are still not commercialized and in development or in a prototype phase. Due to this, the project is dependent on these technologies being developed further and commercialized before the project is possible to realize. Given the calculation of NPV in Section 8, the project is economically feasible. However, it must be added that the economical analysis is only a rough estimate of the actual costs and income.

In our investigations we have not finished the execution of the design for the fresh water supply needed in the hydrogen production. Hence, it is recommended that further investigations should be done, especially since this may be a defining part for the magnitude of the energy demand. Further work is also recommended in the CO<sub>2</sub> removal design. Technologies such as SMR membrane reactors for simultaneous separation of H<sub>2</sub> and sorption of CO<sub>2</sub> is highlighted as a promising concept.

Before the project can be launched a deeper analysis of the solution must be done. This report only gives an introduction to how this project can be done. For further development detailed analysis regarding all the components must be done. For the CCS part of the project a lot of data must be collected, such as 3D seismic surveys. This has not been taken into account when analysing the economic part of the project.

---

## Bibliography

- [1] Equinor. *2022 Energy Transition Plan*. URL: <https://www.equinor.com/content/dam/statoil/documents/sustainability/energy-transition-plan-2022-equinor.pdf> (visited on 19th Apr. 2022).
- [2] J.-O. Koch and O.R. Heum. ‘Exploration trends of the Halten Terrace’. In: *Petroleum Exploration and Exploitation in Norway*. Ed. by S. Hanslien. Vol. 4. Norwegian Petroleum Society Special Publications. Elsevier, 1995, pp. 235–251. DOI: [https://doi.org/10.1016/S0928-8937\(06\)80044-5](https://doi.org/10.1016/S0928-8937(06)80044-5). URL: <https://www.sciencedirect.com/science/article/pii/S0928893706800445>.
- [3] Richard Rwechungura and Nan Cheng. *Lecture Slides - TPG 4851*. 2022.
- [4] Norwegian Petroleum Directorate. *Skuld*. URL: <https://www.norskpetroleum.no/fakta/felt/skuld/> (visited on 20th Apr. 2022).
- [5] Norwegian Petroleum Directorate. *Norne*. URL: <https://www.norskpetroleum.no/fakta/felt/norne/> (visited on 20th Apr. 2022).
- [6] Norwegian Petroleum Directorate. *Alve*. URL: <https://www.norskpetroleum.no/fakta/felt/alve/> (visited on 20th Apr. 2022).
- [7] Norwegian Petroleum Directorate. *Marulk*. URL: <https://www.norskpetroleum.no/fakta/felt/marulk/> (visited on 20th Apr. 2022).
- [8] Norwegian Petroleum Directorate. *Skarv*. URL: <https://www.norskpetroleum.no/fakta/felt/skarv/> (visited on 20th Apr. 2022).
- [9] Norwegian Petroleum Directorate. *Heidrun*. URL: <https://www.norskpetroleum.no/fakta/felt/heidrun/> (visited on 20th Apr. 2022).
- [10] Norwegian Petroleum Directorate. *Asgard*. URL: <https://www.norskpetroleum.no/fakta/felt/asgard/> (visited on 20th Apr. 2022).
- [11] Norwegian Petroleum Directorate. *Morvin*. URL: <https://www.norskpetroleum.no/fakta/felt/morvin/> (visited on 20th Apr. 2022).
- [12] Norwegian Petroleum Directorate. *Kristin*. URL: <https://www.norskpetroleum.no/fakta/felt/kristin/> (visited on 20th Apr. 2022).
- [13] Norwegian Petroleum Directorate. *Yttergryta*. URL: <https://www.norskpetroleum.no/fakta/felt/yttergryta/> (visited on 20th Apr. 2022).
- [14] Norwegian Petroleum Directorate. *Tyrihans*. URL: <https://www.norskpetroleum.no/fakta/felt/tyrihans/> (visited on 20th Apr. 2022).
- [15] Norwegian Petroleum Directorate. *Mikkel*. URL: <https://www.norskpetroleum.no/fakta/felt/mikkel/> (visited on 20th Apr. 2022).
- [16] Norwegian Petroleum Directorate. *Draugen*. URL: <https://www.norskpetroleum.no/fakta/felt/draugen/> (visited on 20th Apr. 2022).
- [17] Norwegian Petroleum Directorate. *Njord*. URL: <https://www.norskpetroleum.no/fakta/felt/njord/> (visited on 20th Apr. 2022).
- [18] Norwegian Petroleum Directorate. *Hyme*. URL: <https://www.norskpetroleum.no/fakta/felt/hyme/> (visited on 20th Apr. 2022).
- [19] Norwegian Petroleum Directorate. *NPD Fields*. URL: <https://www.norskpetroleum.no/fakta/felt/> (visited on 20th Apr. 2022).
- [20] Equinor. *Offshore wind power in the UK*. URL: <https://www.equinor.com/en/what-we-do/uk-wind.html> (visited on 17th Apr. 2022).
- [21] Equinor. *Hywind Tampen*. URL: <https://www.equinor.com/en/what-we-do/hywind-tampen.html> (visited on 17th Apr. 2022).
- [22] GE Renewable Energy. *Haliade-X offshore wind turbine*. URL: <https://www.ge.com/renewableenergy/wind-energy/offshore-wind/haliade-x-offshore-turbine> (visited on 17th Apr. 2022).
- [23] Stefan Pfenninger and Iain Staffell. *Renewable Ninja*. URL: <https://www.renewables.ninja/> (visited on 17th Apr. 2022).

- 
- [24] FLASC B.V. *FLASC*. URL: <https://www.offshoreenergystorage.com/> (visited on 14th Mar. 2022).
- [25] Hydrogen and Fuel Cell Technologies Office. *Hydrogen Production: Natural Gas Reforming*. URL: <https://www.energy.gov/eere/fuelcells/hydrogen-production-natural-gas-reforming> (visited on 15th Feb. 2022).
- [26] Air Liquide. *Autothermal Reforming (ATR) - Syngas Generation*. URL: <https://www.engineering-airliquide.com/autothermal-reforming-atr-syngas-generation> (visited on 15th Feb. 2022).
- [27] A. Nieto-Márquez et al. ‘Autothermal reforming and water–gas shift double bed reactor for H<sub>2</sub> production from ethanol’. In: *Chemical Engineering and Processing: Process Intensification* 74 (2013), pp. 14–18. ISSN: 0255-2701. DOI: <https://doi.org/10.1016/j.cep.2013.10.006>. URL: <https://www.sciencedirect.com/science/article/pii/S025527011300247X>.
- [28] Madhu. *Difference Between Steam Reforming and Autothermal Reforming*. URL: <https://www.differencebetween.com/difference-between-steam-reforming-and-autothermal-reforming/> (visited on 15th Feb. 2022).
- [29] James G. Speight. ‘Chapter 5 - The Fischer-Tropsch Process’. In: *Gasification of Unconventional Feedstocks*. Ed. by James G. Speight. Boston: Gulf Professional Publishing, 2014, pp. 118–134. ISBN: 978-0-12-799911-1. DOI: <https://doi.org/10.1016/B978-0-12-799911-1.00005-4>. URL: <https://www.sciencedirect.com/science/article/pii/B9780127999111000054>.
- [30] R. A. Wood et al. *HTGR-Integrated Hydrogen Production via Steam Methane Reforming (SMR) Process Analysis*. Idaho National Laboratory, 2010.
- [31] Rain Saulnier, Keith Minnich and P. Kim Sturgess. ‘Water for the Hydrogen Economy’. In: (Nov. 2020).
- [32] Jungbin Kim et al. ‘A comprehensive review of energy consumption of seawater reverse osmosis desalination plants’. In: *Applied Energy* 254 (2019), p. 113652. ISSN: 0306-2619. DOI: <https://doi.org/10.1016/j.apenergy.2019.113652>. URL: <https://www.sciencedirect.com/science/article/pii/S030626191931339X>.
- [33] Dan Sadler et al. *H21 NoE Report/2018*. Tech. rep. Northern Gas Networks, Equinor and Cadent, 2018.
- [34] MarineTraffic. *SKARV FPSO*. URL: [https://www.marinetraffic.com/no/ais/details/ships/shipid:876354/mmsi:-9433042/imo:9433042/vessel:SKARV\\_FPSO](https://www.marinetraffic.com/no/ais/details/ships/shipid:876354/mmsi:-9433042/imo:9433042/vessel:SKARV_FPSO) (visited on 3rd May 2022).
- [35] Barbara Uliasz, Misiak Joanna Lewandowska and Śmierzchalska Rafal Matuła. ‘Criteria for selecting sites for integrated CO<sub>2</sub> storage and geothermal energy recovery’. In: *Elsevier* 258 (Feb. 2021). DOI: 124822.
- [36] Reidulv Bøe et al. ‘CO<sub>2</sub> point sources and subsurface storage capacities for CO<sub>2</sub> in aquifers in Norway’. In: *NGU, EU* (Sept. 2002), p. 132.
- [37] Eva K. Halland, Jasminka Mujezinović and Fridtjof Riis. *CO<sub>2</sub> Storage Atlas*. Norwegian Petroleum Directorate, 2014.
- [38] Karen L. Anthonsen and Gry Møl Mortensen, Sandra Ó. Snæbjörnsdóttir and Yuefeng Gao. *Compilation of GIS-data for all Nordic Countries*. Tech. rep. Norway: Nordic CCS Competence center, Mar. 2015.
- [39] M. K. Jha. *Aquifer and Its Properties*. URL: <http://ecoursesonline.iasri.res.in/mod/page/view.php?id=1814> (visited on 19th Apr. 2022).
- [40] Matteo Loizzo et al. ‘Reusing O&G-Depleted Reservoirs for CO<sub>2</sub> Storage: Pros and Cons’. In: *SPE Projects Facilities & Construction* 5 (Sept. 2010), pp. 166–172. DOI: 10.2118/124317-PA.
- [41] Auli Niemi, Jacob Bear, Jacob Bensabat et al. *Geological storage of CO<sub>2</sub> in deep saline formations*. Vol. 29. Springer, 2017.
- [42] Philip Ringrose. *How to Store CO<sub>2</sub> Underground: Insights from early-mover CCS Projects*. Jan. 2020. ISBN: 978-3-030-33112-2. DOI: 10.1007/978-3-030-33113-9.
- [43] Anne-Kari Furre et al. ‘Planning deep subsurface CO<sub>2</sub> storage monitoring for the Norwegian full-scale CCS project’. In: *First Break* 38.10 (2020), pp. 55–60.

- 
- [44] Office of energy efficiency and U.S. Department of Energy renewable energy. *Hydrogen Pipelines*. URL: <https://www.energy.gov/eere/fuelcells/hydrogen-pipelines> (visited on 19th Apr. 2022).
- [45] Gassco. *Haltenpipe*. URL: <https://www.gassco.no/en/our-activities/pipelines-and-platforms/haltenpipe/> (visited on 19th Apr. 2022).
- [46] M W Melaina, O Antonia and M Penev. *Blending Hydrogen into Natural Gas Pipeline Networks: A Review of Key Issues*. Tech. rep. Mar. 2013. DOI: 10.2172/1068610. URL: <https://www.osti.gov/biblio/1068610>.
- [47] Current Research Information System in Norway. *Safe Pipelines for Hydrogen Transport*. URL: <https://app.cristin.no/projects/show.jsf?id=2062917> (visited on 10th Apr. 2022).
- [48] Norwegian Petroleum Directorate. *NPD FactMaps*. URL: [https://factmaps.npd.no/factmaps/3\\_0/](https://factmaps.npd.no/factmaps/3_0/) (visited on 20th Apr. 2022).
- [49] Antonin Chapoy et al. 'Effect of impurities on thermophysical properties and phase behaviour of a CO<sub>2</sub>-rich system in CCS'. In: *International Journal of Greenhouse Gas Control* 19 (2013), pp. 92–100.
- [50] Energy transition. *LCO<sub>2</sub> Carriers indispensable for long-distance transport*. URL: <https://solutions.mhi.com/ccus/lco2-carrier/> (visited on 19th Apr. 2022).
- [51] Christine Röckmann, Sander Lagerveld and John Stavenuiter. 'Operation and Maintenance Costs of Offshore Wind Farms and Potential Multi-use Platforms in the Dutch North Sea'. In: Apr. 2017, pp. 97–113. ISBN: 978-3-319-51157-3. DOI: 10.1007/978-3-319-51159-7\_4.
- [52] Jonah Ury. *Opex is being overvalued as a driver of the future price of offshore wind*. URL: <https://www.rechargenews.com/markets/opex-is-being-overvalued-as-a-driver-of-the-future-price-of-offshore-wind/2-1-960661> (visited on 19th Apr. 2022).
- [53] Equinor. *Industrialising floating offshore wind*. URL: <https://www.equinor.com/en/what-we-do/floating-wind.html> (visited on 17th Apr. 2022).
- [54] GWPF Andrew Montford. *Hywind, low economics: The cost of floating offshore wind power*. URL: <https://www.netzerowatch.com/hywind-low-economics/> (visited on 19th Apr. 2022).
- [55] Renewables Reuters Events. *Equinor cuts floating wind costs by 40% in design revamp*. URL: <https://www.reutersevents.com/renewables/wind-energy-update/equinor-cuts-floating-wind-costs-40-design-revamp> (visited on 19th Apr. 2022).
- [56] Arne Eik. *How to reach 40-60 Euro per MWh for floating offshore wind in 2030?* [https://www.uib.no/sites/w3.uib.no/files/attachments/2019-09-12\\_how\\_to\\_get\\_to\\_40-60\\_science\\_meets\\_industry\\_bergen\\_.pdf](https://www.uib.no/sites/w3.uib.no/files/attachments/2019-09-12_how_to_get_to_40-60_science_meets_industry_bergen_.pdf). Accessed: 2022-04-19. 2019.
- [57] Dominique Reverdy and Ivan Skenderoski. *Submarine Cables: Structuring and Financing Options*. Tech. rep. Dubai, United Arab Emirates: Salience Consulting DMCC, Jan. 2015.
- [58] Wesley Cole, A. Will Frazier and Chad Augustine. *Cost Projections for Utility-Scale Battery Storage: 2021 Update*. Tech. rep. NREL/TP-6A20-79236. 15013 Denver West Parkway, USA: National Renewable Energy Laboratory, USA, June 2021.
- [59] Hesty Kurniawati, Wasis Aryawan and Ahmad Baidowi. 'LONG-TERM FSO/FPSO CHARTER RATE ESTIMATION'. In: *Kapal* 13 (Feb. 2016). DOI: 10.12777/kpl.13.1.7-12.
- [60] Tan-Ping Chen. 'Hydrogen Delivey Infrastructure Option Analysis'. In: (May 2010). DOI: 10.2172/982359. URL: <https://www.osti.gov/biblio/982359>.
- [61] Magnus Killingland, Matias Krogh Boge and Guido Magneschi. *Potential for reduced costs for carbon capture, transport and storage value chains (CCS)*. Tech. rep. Norway: DNV GL Energy, Feb. 2020.
- [62] European Technology Platform for Zero Emission Fossil Fuel Power Plants. *The Costs of CO<sub>2</sub> Transport*. Tech. rep. URL: <https://www.globalccsinstitute.com/archive/hub/publications/119811/costs-co2-transport-post-demonstration-ccs-eu.pdf>.
- [63] Hydrogen Valley Platform. *Hydrogen cost and sales prices*. URL: <https://www.h2v.eu/analysis/statistics/financing/hydrogen-cost-and-sales-prices> (visited on 29th Apr. 2022).
- [64] Trading Economics. *EU Carbon Permits*. URL: <https://tradingeconomics.com/commodity/carbon> (visited on 19th Apr. 2022).
-

- 
- [65] Taran Fæhn and Kevin Kaushal. *Økonomien i regjeringens klimaplan mot 2030*. URL: <https://www.ssb.no/natur-og-miljo/artikler-og-publikasjoner/okonomien-i-regjeringens-klimaplan-mot-2030> (visited on 19th Apr. 2022).
  - [66] NPD. *Geology of the Norwegian Sea*. URL: <https://www.npd.no/en/facts/publications/co2-atlases/co2-atlas-for-the-norwegian-continental-shelf/5-the-norwegian-sea/5.1-geology-of-the-norwegian-sea/> (visited on 19th Apr. 2022).
  - [67] Norwegian Petroleum Directorate. *NPD Fact page*. URL: <https://factpages.npd.no/no/strat/PageView/Litho/Formations/48> (visited on 20th Apr. 2022).

# Appendix

## A Infrastructure in the Haltenbanken Area

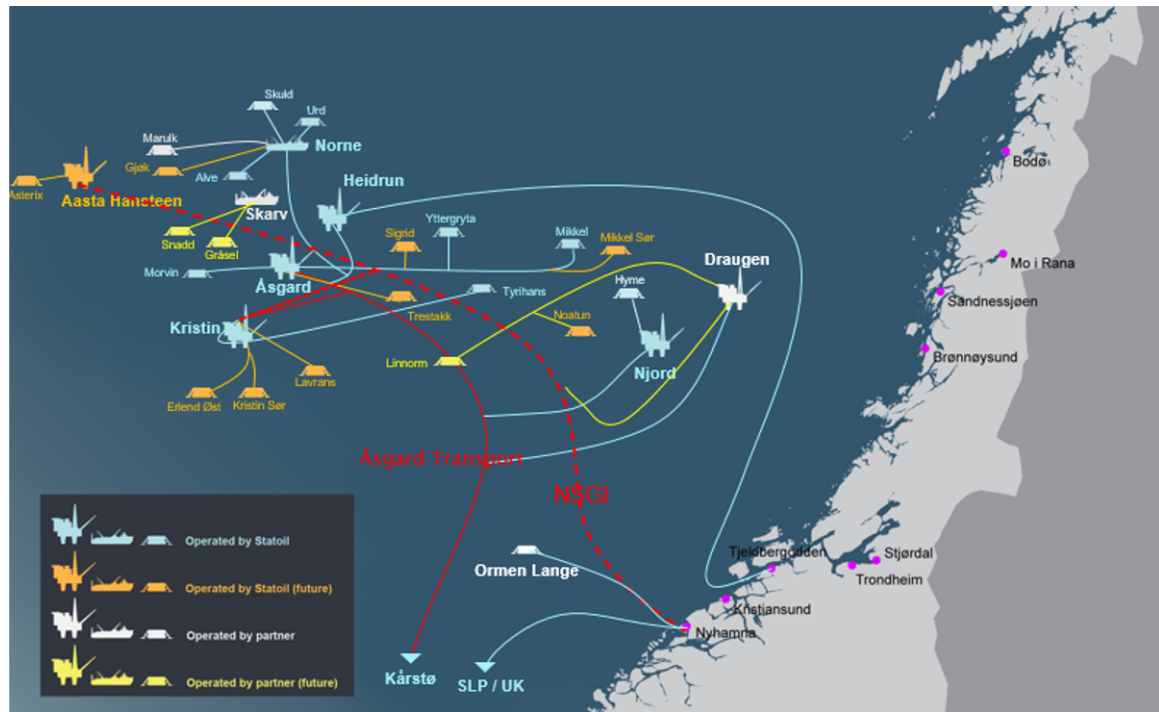


Figure 18: Infrastructure of the Halten Terrace.

Source: [3]

## B Lithostratigraphy of the Haltenbanken Area

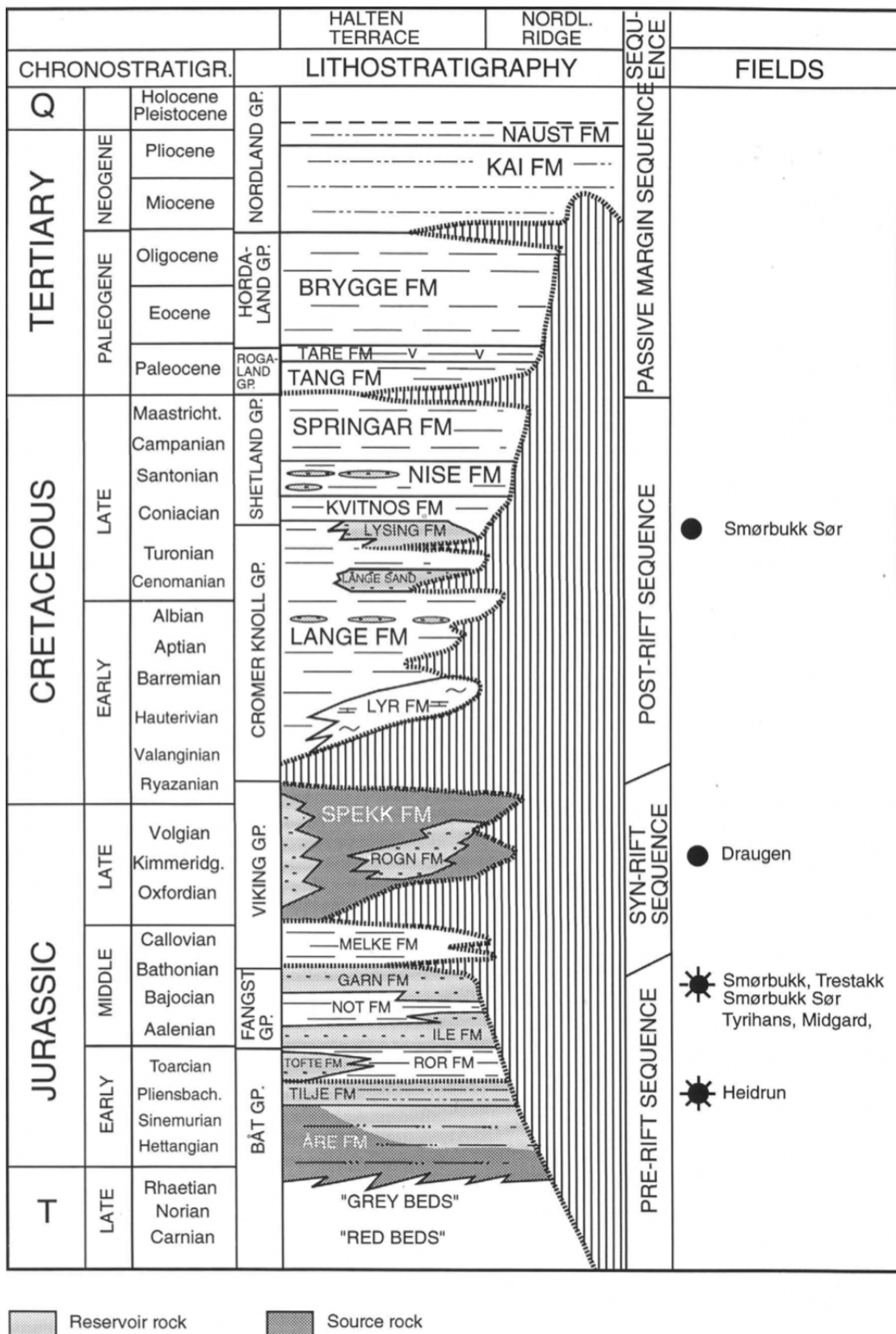


Figure 19: General stratigraphy and hydrocarbon occurrences of the Halten Terrace.

Source: [2]

## C Calculations - Excel

Energy content from hydrogen					
Year [-]	Hydrogen gas per day [Mill m <sup>3</sup> at normal pressure ]	Energy from Hydrogen		Energy with 30 % transformation	
		[kWh per day]	[GWh per year]	[kWh per day]	[GWh per year]
1997	2.36	6588723	2405	1976617	721
1998	4.13	11517590	4204	3455277	1261
1999	4.66	12994045	4743	3898214	1423
2000	8.38	23382423	8535	7014727	2560
2001	47.69	133104016	48583	39931205	14575
2002	68.09	190020549	69358	57006165	20807
2003	92.60	258434285	94329	77530285	28299
2004	103.77	289600911	105704	86880273	31711
2005	105.92	295585273	107889	88675582	32367
2006	113.53	316834560	115645	95050368	34693
2007	134.40	375079552	136904	112523866	41071
2008	146.91	410000032	149650	123000010	44895
2009	153.97	429688126	156836	128906438	47051
2010	143.58	400700860	146256	120210258	43877
2011	141.26	394218411	143890	118265523	43167
2012	134.78	376140579	137291	112842174	41187
2013	137.08	382560273	139634	114768082	41890
2014	155.01	432580745	157892	129774223	47368
2015	161.27	450068305	164275	135020492	49282
2016	158.77	443087508	161727	132926252	48518
2017	171.35	478187070	174538	143456121	52361
2018	157.20	438704465	160127	131611340	48038
2019	151.97	424097715	154796	127229315	46439
2020	133.97	373868644	136462	112160593	40939

Figure 20: Energy content of hydrogen.

Energy demand for transformation from natural gas (methan) to hydrogen										
Year	Natural gas per day [10 <sup>3</sup> Mill]	Hydrogen gas per day [Mill m <sup>3</sup> at normal pressure]	Hydrogen gas per day [MMSCFD (mill standard cubic feet)]	Captured CO <sub>2</sub> gas [Tonnes/day]	30% CO <sub>2</sub> gas [Mill tonnes/year]	Energy demand for 100% transformation [MW per day]	Energy demand for 30% transformation [GWh per year]	Energy demand for 30% transformation [MW per day]	Amount of windmills [-]	
1997	1.56	0.89	2	83	1374	0.13	9	81	24	0.4
1998	1.76	4	4	146	2403	0.26	16	141	42	0.7
1999	1.76	5	5	164	2711	0.30	18	160	5	0.8
2000	3.17	8	296	4878	0.53	33	287	10	86	1.4
2001	18.07	48	1684	27766	3.04	187	1634	56	490	7.8
2002	25.79	68	2405	39638	4.34	266	2333	80	700	11.1
2003	35.08	93	3270	53909	5.90	362	3173	109	952	15.1
2004	39.31	104	3665	60411	6.61	406	3556	122	1067	16.9
2005	40.12	106	3740	61659	6.75	414	3629	124	1089	17.3
2006	43.00	114	4099	66092	7.24	444	3890	133	1167	18.5
2007	50.91	134	4746	78242	8.57	526	4606	158	1382	21.9
2008	55.65	147	5188	85526	9.37	575	5034	172	1510	24.0
2009	58.32	154	5437	88633	9.81	602	5276	181	1583	25.1
2010	54.39	144	5071	83586	9.15	562	4920	168	1476	23.4
2011	53.51	141	4989	82234	9.00	553	4841	166	1452	23.1
2012	51.05	135	4760	78463	8.59	527	4619	158	1386	22.0
2013	51.93	137	4841	79802	8.74	536	4697	161	1409	22.4
2014	58.71	155	5474	90237	9.88	606	5312	182	1593	25.3
2015	61.09	161	5695	93884	10.28	631	5526	189	1658	26.3
2016	60.14	159	5607	92428	10.12	621	5441	186	1632	25.9
2017	64.50	171	6051	95750	10.92	670	5872	201	1761	28.0
2018	59.55	157	5551	91514	10.02	615	5387	184	1616	25.7
2019	57.56	152	5367	88467	9.69	594	5207	178	1562	24.8
2020	50.75	134	4731	77989	8.54	524	4591	157	1377	21.9

Figure 21: Energy demand for methane conversion.

## D Tables and Images regarding CCS

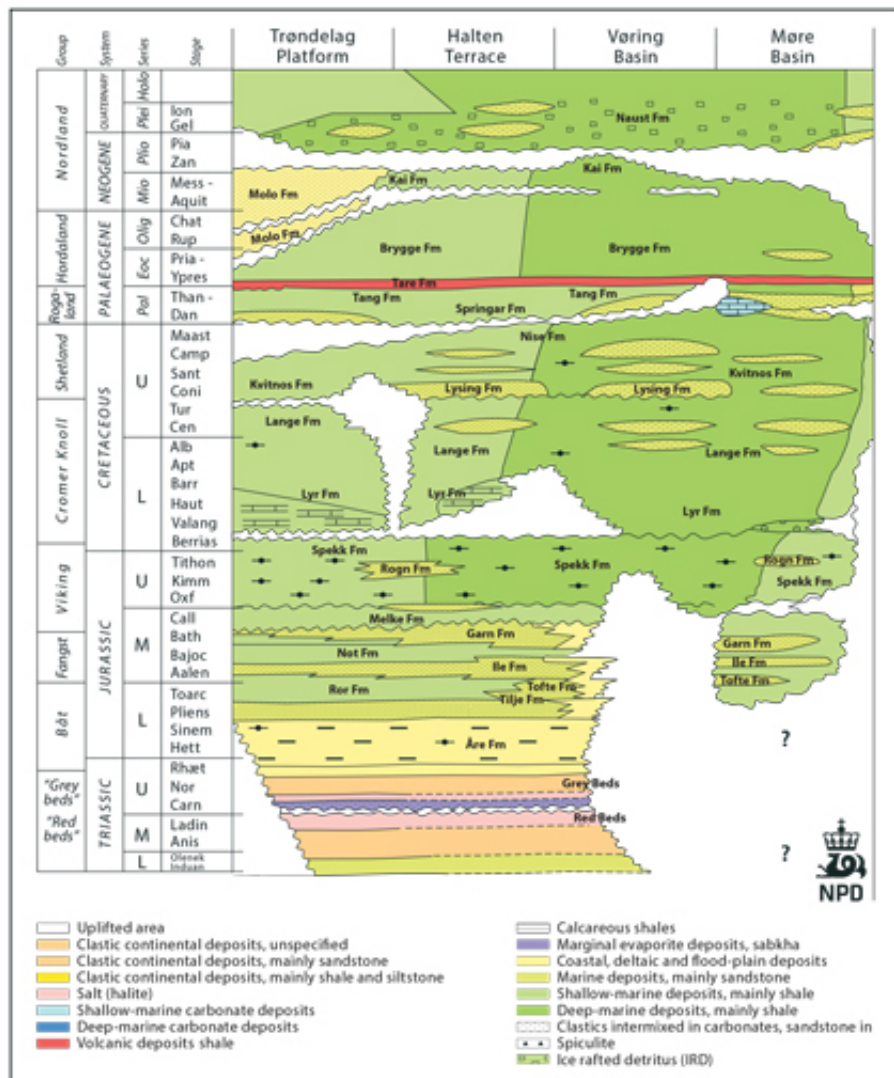


Figure 22: General stratigraphy of the Norwegian Sea.

Source: [66]

The Tilje/Are Aquifer		
Storage system		Closed
Rock Volume		9200 Gm <sup>3</sup>
Net volume		2700 Gm <sup>3</sup>
Pore volume		900 Gm <sup>3</sup>
Average depth		1940 m
Average Net/gross		0.3
Average porosity		0.21
Average permeability		140 mD
Storage efficiency		0.70%
Storage capacity aquifer		4.0 Gt
Reservoir quality	Capacity	2
	Injectivity	2
Seal quality	Seal	3
	Fractured seal	2
	wells	3

Table 11: The Tijle/Are Aquifer Features.

Source: [37]

The Garn/Ile Aquifer			
		half open	closed
Storage system			
Rock Volume		4400 Gm <sup>3</sup>	4400 Gm <sup>3</sup>
Net volume		1100 Gm <sup>3</sup>	1100 Gm <sup>3</sup>
Pore volume		300 Gm <sup>3</sup>	300 Gm <sup>3</sup>
Average depth Garn Fm		1675 m	1675 m
Average depth Ile Fm		1825 m	1825 m
Average Net/gross		0.25	0.25
Average porosity		0.27	0.27
Average permeability		580 mD	580 mD
Storage efficiency		4.00%	0.20%
Storage capacity aquifer		8 Gt	0.4 Gt
Reservoir quality	Capacity	2	2
	Injectivity	3	3
Seal quality	Seal	3	3
	Fractured seal	3	3
	wells	3	3

Table 12: The Garn/Ile Aquifer Features.

Source: [37]

Injectivity in Garn Formation in Ile/Garn Aquifer		
Bottom of Garn (TVD)	m	2061.000
Pore Pressure Gradient	sg	1.010
Reservoir Pressure at bottom of Fensfjord	Psi	2955.886
	Bar	203.854
Fracture Gradient	sg	1.630
Fracture Pressure at bottom of Fensfjord	Psi	4770.391
	bar	328.992
95% of Fracture Pressure (safety Margin)	Psi	4531.871
Reservoir Temperature	C	146.000
CO2 Density	Kg/m3	345.000
Wellhead Pressure, Pwh	bar	243.000
Bottom hole Pressure, Pbh	bar	312.754
	Psi	4534.926
Horizontal permeability, $k_h$	md	580.000
Vertical permeability, $k_v$	md	580.000
Layer thickness, h	m	120.000
Pore Volume	m3	540000.000
Porosity		0.200
Reservoir top area	m2	22500.000
Reservoir pressure, $p_R$	bara	203.854
Bottom-hole pressure, $p_{wh}$	bara	312.754
$p_{av}$	bara	258.304
CO2 viscosity, $\mu_o$ at average pressure	cp	0.0412
CO2 volume factor, $B_o$ , at average pressure	m3/Sm3	0.420
Wellbore radius, $r_w$	m	0.150

Table 13: Parameters used in the well design. All data are compiled from NPD website.

Source: [67]

Results - Vertical Wells		
External radius, $r_e$	m	84.628
Skin, s		0.000
Shape factor, $s_A$		0.000
Injectivity Index, J	Sm3/d/bar	38550.706
	Sm3/d	4198144.622
Injection Rate, q	Ton/d	7547.905
	Ton/year	2754985.233
Target CO2 Injection	Ton/year	10000000.000
Total number of Wells		4.000

Table 14: Results for the well design.

---

## E Table of Estimated Costs and Income

	CAPEX [MNOK]	OPEX [MNOK]
<b>COSTS</b>		
Windmills	14 318	4 295
Energy Storage	853	85
Power cable	1 163	70
Hydrogen Facility	64 358	2 153
Vessel		Included in NPV
Hydrogen transport	9 248	462
CCS		
Transportation	3 420	529
Storage	54 750	1 670
Extra margin	14 811	926
<b>INCOME</b>		
Hydrogen sales		37 486
CO2 quotas		1 380
<b>TOTAL</b>	<b>- 162 921</b>	<b>28 675</b>

Table 15: Calculated CAPEX and OPEX, in MNOK (2022).

RATES USED					
	Conversion rate	Inflation rate		Discount rate	
\$ to NOK	9.14	US \$ 2020-2022	1.11	10 %	
£ to NOK	11.63	US \$ 2016-2022	1.20		
€ to NOK	9.72	£ 2018 - 2022	1.10		
WINDMILL FARM					
Windmills					
	Amount	Total capacity	Price	CAPEX	OPEX
	[ <sup>-</sup> ]	[MW]	[MNOK/MW]	[MNOK]	[MNOK]
	28	336	43	14 318	4 295
Power Cable					
	Distance	Price	CAPEX	OPEX	
	[km]	[mill £/km]	[MNOK]	[MNOK]	
	40	2.50	1 163	70	
Energy Storage					
	Amount	Capacity	price	CAPEX	OPEX, 10%
	[ <sup>-</sup> ]	[MWh/piece]	[MWh]	[2020 \$/kWh]	[MNOK]
	28	10	280	300	853
					85
CCS					
Storage					
	0.8Mtpa		8 Mtpa		
	CAPEX	OPEX	CAPEX	OPEX	
	[MNOK]	[MNOK]	[MNOK]	[MNOK]	
	5 475	167	54 750	1 670	
Transportation					
	Distance	Capacity	Price	OPEX	Price
	[km]	[Mtpa]	[€/tonnes CO2]	[MNOK]	[MNOK/km]
	180	8.00	6.81	529	19
					3 420
HYDROGEN					
Production facility					
	H21 info for scaling:		Capacity	CAPEX	OPEX
			[MW]	[M £ 2018]	[M £ 2018]
			12.15	8 520	285
	Capacity	CAPEX	OPEX		
	[MW]	[MNOK]	[MNOK]		
	7.15	64 358	2 153		
Vessel					
Renting price:					
	US \$ (2016)				
	per day	per year (0-10)	per year (10-15)	per year (15-20)	
	27 500	10 037 500	5 018 750	3 011 250	
	NPV for 20 years	Average			
Transport					
	Distance	Price	CAPEX	OPEX	
	[km]	[MNOK/km]	[MNOK]	[MNOK]	
	443	21	9 248	462	
INCOME					
Hydrogen sales					
	Amount	Price	Income		
	[mill kg per year]	[€/kg]	[NOK/kg]	[MNOK/year]	
	1 286	3.00	29.16	37 486	
CO2 quotas					
	71 % CO2	Carbon price	Income		
	[tonnes]	[€/tonnes]	[MNOK/year]		
	1 775 000	80	1 380		

Figure 23: Overview of calculation of the estimated costs and income, in MNOK (2022).